



HAL
open science

Bayesian Calibration in a multi-output transposition context

Gilles Defaux, Cédric Durantin, Josselin Garnier, Baptiste Kerleguer,
Guillaume Perrin, Charlie Sire

► **To cite this version:**

Gilles Defaux, Cédric Durantin, Josselin Garnier, Baptiste Kerleguer, Guillaume Perrin, et al..
Bayesian Calibration in a multi-output transposition context. 2024. hal-04717715

HAL Id: hal-04717715

<https://hal.science/hal-04717715v1>

Preprint submitted on 18 Nov 2024

HAL is a multi-disciplinary open access archive for the deposit and dissemination of scientific research documents, whether they are published or not. The documents may come from teaching and research institutions in France or abroad, or from public or private research centers.

L'archive ouverte pluridisciplinaire **HAL**, est destinée au dépôt et à la diffusion de documents scientifiques de niveau recherche, publiés ou non, émanant des établissements d'enseignement et de recherche français ou étrangers, des laboratoires publics ou privés.

BAYESIAN CALIBRATION IN A MULTI-OUTPUT TRANSPOSITION CONTEXT

Gilles Defaux,³ Cédric Durantin,³ Josselin Garnier,² Baptiste Kerleguer,³ Guillaume Perrin,⁴ & Charlie Sire^{1,2,*}

¹Inria Saclay Centre, Palaiseau, France

²CMAP, Ecole polytechnique, Institut Polytechnique de Paris, Palaiseau, France

³CEA, DAM, DIF, F-91297 Arpaçon, France

⁴COSYS, Université Gustave Eiffel, Marne-La-Vallée, France

*Address all correspondence to: Charlie Sire, Inria Saclay Centre, Palaiseau, France, E-mail: sire.charlie971@gmail.com

Original Manuscript Submitted: mm/dd/yyyy; Final Draft Received: mm/dd/yyyy

Bayesian calibration is an effective approach for ensuring that numerical simulations accurately reflect the behavior of physical systems. However, because numerical models are never perfect, a discrepancy known as model error exists between the model outputs and the observed data, and must be quantified. Conventional methods can not be implemented in transposition situations, such as when a model has multiple outputs but only one is experimentally observed. To account for the model error in this context, we propose augmenting the calibration process by introducing additional input numerical parameters through a hierarchical Bayesian model, which includes hyperparameters for the prior distribution of the calibration variables. Importance sampling estimators are used to avoid increasing computational costs. Performance metrics are introduced to assess the proposed probabilistic model and the accuracy of its predictions. The method is applied on a computer code with three outputs that models the Taylor cylinder impact test. The outputs are considered as the observed variables one at a time, to work with three different transposition situations. The proposed method is compared with other approaches that embed model errors to demonstrate the significance of the hierarchical formulation.

KEY WORDS: Bayesian inference, Code transposition, Hierarchical model, Model error, Model calibration, Uncertainty Quantification, Markov Chain Monte Carlo

1. INTRODUCTION

Numerical simulations are increasingly used to understand and optimize complex physical systems, as they enable the prediction of behavior in previously unobserved scenarios. For accurate predictions, the input parameters of these simulations must be carefully specified. Some of the simulation inputs, known as control variables, replicate experimental conditions chosen by the experimenter and are denoted by \mathbf{x} , while others are unknown parameters specific to the computer code, denoted by λ . These parameters typically have a physical significance and must be calibrated to ensure the code predictions closely match the actual system behavior, observed from limited experimental data. The parameters λ can also be numerical parameters that are needed to run the code. The simplest approach involves performing an optimization scheme on λ to minimize a given distance between observed data and model outputs, see [1–3], then using the optimal values

as if they were known. However, this method assumes no uncertainty in the observed data (no measurement error) and in the code prediction (no model error), which is unrealistic in practice.

A Bayesian methodology that considers noisy observations and treats the unknown parameters as a random vector Λ can be adopted. The a priori density of Λ and the observations are used to build the posterior distribution of Λ , which captures the uncertainty and allows for a predictive distribution of the output. This framework is thoroughly presented in [4] and further studied in numerous works, for example [5–7].

Nevertheless, predicting the behavior of physical systems using numerical models is never perfect, even with well-identified parameter values. There is always a discrepancy between the model outputs and the observed data, which must be accounted for as a model error, as highlighted in various works, see [8–11]. Typically, as detailed in [4], the model error term can be explicitly represented as an additive Gaussian process, with hyperparameters estimated from the observed data. This approach is particularly useful but cannot be implemented in some situations due to the impossible estimation of the hyperparameters. These situations arise when the output of interest does not directly correspond to the experimental data, such as when calibration must be performed based on different experiments not directly suited to the objective. The framework introduced in this paper will be called transposition. Four cases can be identified:

1. Change of scale: The calibration domain is different from the domain of interest of the code.
2. New inputs: The code is calibrated with fewer inputs than it will use.
3. New code: The calibration parameters will be used in another code.
4. Unobserved outputs: The calibration will be carried out by observing some outputs, not all of them.

In this paper, only the case of unobserved outputs will be considered, although the presented method is general enough to be adapted to many transposition scenarios.

A collection of T different output variables of interest is identified and denoted by \mathbf{y} . It depends on control variables $\mathbf{x} \in \mathcal{X}$, with \mathcal{X} a subset of \mathbb{R}^s , $s \in \mathbb{N}^*$, such that:

$$\mathbf{y}(\mathbf{x}) = (y_t(\mathbf{x}))_{t=1}^T \in \mathbb{R}^T.$$

Let \mathbf{f} be a numerical code to compute this T -dimensional output. Its input variables are \mathbf{x} and p unknown physical calibration parameters $\boldsymbol{\lambda} = (\lambda_i)_{i=1}^p \in \mathcal{L} \subset \mathbb{R}^p$, and

$$\mathbf{f}(\mathbf{x}, \boldsymbol{\lambda}) = (f_t(\mathbf{x}, \boldsymbol{\lambda}))_{t=1}^T \in \mathbb{R}^T.$$

The experimental phase is assumed to provide n observations but only for the variable t' , where $1 \leq t' \leq T$. They form the vector $\mathbf{y}_{t', \text{obs}} = (y_{t', \text{obs}, j})_{j=1}^n$ which we consider as realizations of noisy measurements of $y_{t'}$ at design points $\mathbb{X} = (\mathbf{x}_j)_{j=1}^n$ with output measurement error $\mathbf{E} = (E_j)_{j=1}^n$:

$$\mathbf{Y}_{t', \text{obs}} = (Y_{t', \text{obs}, j})_{j=1}^n = (y_{t'}(\mathbf{x}_j) + E_j)_{j=1}^n \in \mathbb{R}^n. \quad (1)$$

The probability density function (pdf) of the measurement error is known and is denoted by p_E . Note that the true values of control variables are known, no measurement error is considered on these variables. The transposition comes from the fact that only the variable $y_{t'}$ is measured in the experimental phase, while the objective is to predict $y_t(\mathbf{x}_0)$ for $1 \leq t \leq T$, and $\mathbf{x}_0 \in \mathcal{X} \setminus \mathbb{X}$. In the following, and without loss of generality, we assume that the variable y_1 is measured (i.e. $t' = 1$) considering the random vector $\mathbf{Y}_{1, \text{obs}} = (Y_{1, \text{obs}, j})_{j=1}^n = (y_1(\mathbf{x}_j) + E_j)_{j=1}^n$.

The common additive discrepancy to represent the model error would be introduced as follows, by modeling the output variables of interest as $\mathbf{Y}(\mathbf{x}) = (Y_t(\mathbf{x}))_{t=1}^T = \mathbf{f}(\mathbf{x}, \boldsymbol{\Lambda}) + \boldsymbol{\Delta}(\mathbf{x})$, with $\boldsymbol{\Lambda} \in \mathbb{R}^p$ a random vector of pdf p_Λ and $\boldsymbol{\Delta}$ a T -variate Gaussian process with prior information depending on some hyperparameters ϕ . In our transposition context, some of these hyperparameters are impossible to estimate.

Indeed, let us consider for instance $\Delta = (\Delta_t)_{t=1}^T$ pairwise independent Gaussian processes with respective mean $\mu_t(\cdot)$ and covariance $c_t(\cdot, \cdot)$ that depends on hyperparameters ϕ_t . It quickly appears that for every t , experimental measurements of y_t are needed to estimate ϕ_t , but they are not available in our this context.

Therefore, the objective is to propose a model error with hyperparameters that can be estimated from the observations $\mathbf{Y}_{1,\text{obs}}$. As presented in [12], embedded errors can be employed to build a mathematical relationship between the observations and the variables of interest. A similar approach is described in [13], where an embedding $Y_t(\mathbf{x}) = f_t(\mathbf{x}, \Lambda + \Delta)$ is considered with Δ being a random discrepancy whose parameters require calibration, as detailed in Appendix E. In this paper, the embedding differs from this strategy by increasing the variability in the calibration variables Λ through the inclusion of $q - p$ additional numerical parameters to represent the model error, and then work with a q -dimensional vector Λ . A hierarchical description is proposed for these additional parameters, to estimate the hyperparameters of their prior distribution [14].

The article is organized as follows: Section 2 outlines the Bayesian methodology tailored to the transposition context and introduces the surrogate model used. Section 3 describes the application test case and the performance metrics examined, followed by numerical results with a comparison of various approaches, including the method from [13]. Finally, Section 4 summarizes the work and proposes possible extensions.

2. BUILDING AN ADAPTED BAYESIAN FRAMEWORK

2.1 Bayesian calibration

In the Bayesian framework, the idea is to obtain the posterior distribution (i.e. conditioned by the experimental data) of parameters, that balances prior knowledge with observed data, see [15]. More precisely, we consider

$$\begin{cases} Y_t(\mathbf{x}) = f_t(\mathbf{x}, \Lambda), & 1 \leq t \leq T, \mathbf{x} \in \mathcal{X} \\ Y_{1,\text{obs},j} = Y_1(\mathbf{x}_j) + E_j, & 1 \leq j \leq n, \end{cases} \quad (2)$$

with Λ of prior pdf p_Λ and E of known pdf p_E . As explained in Section 1, here we consider $\Lambda \in \mathbb{R}^q$, as we consider the p unknown physical parameters and $q - p$ numerical parameters included to represent the model error. Obviously, the following formulas are valid when considering the classical situation $\Lambda \in \mathbb{R}^p$.

We want to investigate the a posteriori distribution of $Y_t(\mathbf{x}_0)$, i.e., the distribution of $Y_t(\mathbf{x}_0) \mid \mathbf{y}_{1,\text{obs}}$, by estimating $\mathbb{E}(\psi(Y_t(\mathbf{x}_0)) \mid \mathbf{y}_{1,\text{obs}})$ for all $\psi : \mathbb{R} \rightarrow \mathbb{R}$ such that $\mathbb{E}(\psi(Y_t(\mathbf{x}_0)) \mid \mathbf{y}_{1,\text{obs}})$ is defined. In particular, the estimation of $\mathbb{E}(Y_t(\mathbf{x}_0) \mid \mathbf{y}_{1,\text{obs}})$ and $\mathbb{E}(Y_t(\mathbf{x}_0)^2 \mid \mathbf{y}_{1,\text{obs}})$ are required to determine the predictive mean and standard deviation.

The expectation given the observations can be expressed:

$$\mathbb{E}(\psi(Y_t(\mathbf{x}_0)) \mid \mathbf{y}_{1,\text{obs}}) = \int_{\mathbb{R}^q} \psi(f_t(\mathbf{x}_0, \lambda)) p(\lambda \mid \mathbf{y}_{1,\text{obs}}) d\lambda, \quad (3)$$

with $p(\lambda \mid \mathbf{y}_{1,\text{obs}})$ the pdf of the a posteriori distribution of Λ . Bayes' theorem, see [16], gives $p(\lambda \mid \mathbf{y}_{1,\text{obs}}) = \frac{p(\mathbf{y}_{1,\text{obs}} \mid \lambda) p_\Lambda(\lambda)}{\int_{\mathbb{R}^q} p(\mathbf{y}_{1,\text{obs}} \mid \lambda') p_\Lambda(\lambda') d\lambda'}$, where $p(\mathbf{y}_{1,\text{obs}} \mid \lambda) = p_E(\mathbf{y}_{1,\text{obs}} - (f_1(\mathbf{x}_j, \lambda))_{j=1}^n)$ is the likelihood of λ . A consistent estimator of $\mathbb{E}(\psi(Y_t(\mathbf{x}_0)) \mid \mathbf{y}_{1,\text{obs}})$ can be

$$\hat{E}_M(\psi(Y_t(\mathbf{x}_0))) = \frac{1}{M} \sum_{k=1}^M \psi(f_t(\mathbf{x}_0, \Lambda_k)), \quad (4)$$

where $(\Lambda_k)_{k=1}^M$ is sampled with pdf $p(\lambda \mid \mathbf{y}_{1,\text{obs}}) \propto p(\mathbf{y}_{1,\text{obs}} \mid \lambda) p_\Lambda(\lambda)$. However, the normalizing term $\int_{\mathbb{R}^q} p(\mathbf{y}_{1,\text{obs}} \mid \lambda') p_\Lambda(\lambda') d\lambda'$ is known to be intractable in practice, making it impossible to sample directly from $p(\lambda \mid \mathbf{y}_{1,\text{obs}})$ with classical Monte Carlo schemes. Markov Chain Monte Carlo (MCMC) methods are then required here to work with posterior samples $(\Lambda_k)_{k=1}^M$ with pdf proportional to $p(\mathbf{y}_{1,\text{obs}} \mid \cdot) p_\Lambda$. In our study, these MCMC samples are obtained with the Delayed Rejection Adaptive Metropolis (DRAM)

algorithm detailed in [17], but other algorithms such as Hamiltonian Monte Carlo (HMC, [18]) could be used, in particular if q is large.

2.2 Hierarchical model

In the following, $\mathcal{L}_{\text{cal}} \subset \mathbb{R}^p$ is the domain of physical parameters to calibrate, and $\mathcal{L}_{\text{err}} \subset \mathbb{R}^{q-p}$ is the domain of the numerical parameters considered to represent the model error. Then $\lambda \in \mathcal{L}$ is introduced with $\mathcal{L} = \mathcal{L}_{\text{cal}} \times \mathcal{L}_{\text{err}}$. In our study, the $q - p$ numerical parameters in \mathcal{L}_{err} are integrated with a hierarchical description, see [19] and [20], to better target the correct distribution of the parameters of \mathcal{L}_{err} to account for the model error. This is particularly effective even in contexts where measurement noise is significant. The hierarchical description assumes that the a priori distribution of the numerical parameters depends on hyperparameters $\alpha \in \mathcal{A} \subset \mathbb{R}^r$. The pdf of Λ given α is denoted $p_{\Lambda}(\cdot | \alpha)$, and each α drives the numerical parameters for the model error. In a hierarchical description, the objective is to perform Bayesian inference on the hyperparameters α as well, and then consider them as a random variable $\mathbf{A} \in \mathcal{A}$ with prior distribution $p_{\mathbf{A}}$.

As for Equation (3), Bayes' Theorem provides that $p(\alpha | \mathbf{y}_{1,\text{obs}})$, the a posteriori pdf of \mathbf{A} evaluated at α , is proportional to $p(\mathbf{y}_{1,\text{obs}} | \alpha)p_{\mathbf{A}}(\alpha)$, where $p(\mathbf{y}_{1,\text{obs}} | \alpha)$ is the likelihood of α . We have:

$$\mathbb{E}(\psi(\mathbf{Y}_{1,\text{obs}}) | \alpha) = \int_{\mathbb{R}^n} \psi(\mathbf{y}_{1,\text{obs}})p(\mathbf{y}_{1,\text{obs}} | \alpha)d\mathbf{y}_{1,\text{obs}}. \quad (5)$$

Consequently, by using Equation (2), we get

$$\begin{aligned} \mathbb{E}(\psi(\mathbf{Y}_{1,\text{obs}}) | \alpha) &= \int_{\mathbb{R}^n} \int_{\mathbb{R}^q} \psi((f_1(\mathbf{x}_j, \lambda) + \varepsilon_j)_{j=1}^n) p_{\mathbf{E}}(\varepsilon)p(\lambda | \alpha)d\lambda d\varepsilon \\ &= \int_{\mathbb{R}^n} \int_{\mathbb{R}^q} \psi(\mathbf{y}_{1,\text{obs}})p_{\mathbf{E}}(\mathbf{y}_{1,\text{obs}} - (f_1(\mathbf{x}_j, \lambda))_{j=1}^n) p(\lambda | \alpha)d\lambda d\mathbf{y}_{1,\text{obs}} \end{aligned}$$

with the change of variable $\varepsilon \rightarrow \mathbf{y}_{1,\text{obs}} = (f_1(\mathbf{x}_j, \lambda) + \varepsilon_j)_{j=1}^n$. It follows that,

$$\begin{aligned} p(\mathbf{y}_{1,\text{obs}} | \alpha) &= \int_{\mathbb{R}^q} p_{\mathbf{E}}(\mathbf{y}_{1,\text{obs}} - (f_1(\mathbf{x}_j, \lambda))_{j=1}^n) p(\lambda | \alpha)d\lambda \\ &= \mathbb{E}[p(\mathbf{y}_{1,\text{obs}} | \Lambda) | \alpha]. \end{aligned}$$

Thus, the most natural way to estimate $p(\mathbf{y}_{1,\text{obs}} | \alpha)$ for a given α is to compute the Monte Carlo estimator

$$\hat{P}_L(\mathbf{y}_{1,\text{obs}} | \alpha) = \frac{1}{L} \sum_{k=1}^L p(\mathbf{y}_{1,\text{obs}} | \Lambda'_k) \quad (6)$$

with $(\Lambda'_k)_{k=1}^L$ i.i.d. with pdf $p_{\Lambda}(\cdot | \alpha)$.

With this approach, it would lead to $L \times n$ runs of the computer code for the estimation of the likelihood of a single α , which is not feasible in practice.

To save significant computation time, the idea here is to use an Importance Sampling formulation, presented in [21], based on the following result:

$$\begin{aligned} \forall (\alpha, \alpha^*) \text{ such that } \text{supp}(p_{\Lambda}(\cdot | \alpha)) \subset \text{supp}(p_{\Lambda}(\cdot | \alpha^*)), \\ \mathbb{E}[p(\mathbf{y}_{1,\text{obs}} | \Lambda) | \alpha] = \mathbb{E}\left[p(\mathbf{y}_{1,\text{obs}} | \Lambda) \frac{p_{\Lambda}(\Lambda | \alpha)}{p_{\Lambda}(\Lambda | \alpha^*)} | \alpha^*\right] \end{aligned}$$

Then, for all α , we can use the following Importance Sampling estimator of $p(\mathbf{y}_{1,\text{obs}} | \alpha)$, based on sampling associated with the vector of hyperparameters α^* :

Algorithm 1: Iterative estimation of α_{MAP}

Input: \mathbf{A}_0^* , τ
 $\ell \leftarrow 0$, $\nu \leftarrow +\infty$
while $\nu > \tau$ **do**
 Sample $(\Lambda'_k)_{k=1}^L$ i.i.d. with pdf $p_{\Lambda}(\cdot | \mathbf{A}_\ell^*)$
 $\mathbf{A}_{\ell+1}^* \leftarrow \underset{\alpha \in \mathcal{A}}{\operatorname{argmax}} \hat{P}_L^{\mathbf{A}_\ell^*}(\mathbf{y}_{1,\text{obs}} | \alpha) p_{\mathbf{A}}(\alpha)$
 $\nu \leftarrow \|\mathbf{A}_\ell^* - \mathbf{A}_{\ell+1}^*\|$
 $\ell \leftarrow \ell + 1$
end

$$\hat{P}_L^{\alpha^*}(\mathbf{y}_{1,\text{obs}} | \alpha) = \frac{1}{L} \sum_{k=1}^L p(\mathbf{y}_{1,\text{obs}} | \Lambda'_k) \frac{p_{\Lambda}(\Lambda'_k | \alpha)}{p_{\Lambda}(\Lambda'_k | \alpha^*)}, \quad (7)$$

with $(\Lambda'_k)_{k=1}^L$ i.i.d. with pdf $p_{\Lambda}(\cdot | \alpha^*)$. This estimator is consistent and asymptotically normal, as detailed in Section 2.3.

This approach provides estimators of the likelihood of every α with only $n \times L$ runs of the computer code. This allows us to conduct a plug-in strategy by maximizing the a posteriori density of \mathbf{A} and working with the maximum a posteriori $\alpha_{\text{MAP}} = \underset{\alpha \in \mathcal{A}}{\operatorname{argmax}} p(\alpha | \mathbf{y}_{1,\text{obs}})$, or to adopt a full-Bayesian approach and consider the entire posterior distribution of \mathbf{A} with MCMC methods.

2.3 Investigating α_{MAP}

This section details the estimation of α_{MAP} which can then be used as a plug-in value for the hyperparameters to compute $\hat{E}_M(\psi(Y_t(\mathbf{x}_0)))$ with the distribution $p_{\Lambda}(\cdot | \alpha_{\text{MAP}})$ for Λ . The idea is to consider $\hat{P}_L^{\alpha^*}(\mathbf{y}_{1,\text{obs}} | \alpha)$ as the estimator of the likelihood $p(\mathbf{y}_{1,\text{obs}} | \alpha)$ of α , for a relevant α^* as detailed in the following.

2.3.1 Estimation of α_{MAP} .

Theoretically, the maximization of the a posteriori density on \mathcal{A} can be performed by selecting a given α^* and evaluating $\hat{P}_L^{\alpha^*}(\mathbf{y}_{1,\text{obs}} | \alpha) p_{\mathbf{A}}(\alpha)$ for every α . However, the ratios $\frac{p_{\Lambda}(\Lambda'_k | \alpha)}{p_{\Lambda}(\Lambda'_k | \alpha^*)}$ can be highly fluctuating when α is far from α^* , leading to estimators with a high variance. To overcome this issue, the proposed solution is to use an iterative strategy in α^* until reaching a fixed point, as detailed in Algorithm 1. The inputs of the algorithm are \mathbf{A}_0^* , the initial value of α^* and τ , the stop threshold. Note that in this work, the optimization $\mathbf{A}_{\ell+1}^* = \underset{\alpha \in \mathcal{A}}{\operatorname{argmax}} \hat{P}_L^{\mathbf{A}_\ell^*}(\mathbf{y}_{1,\text{obs}} | \alpha) p_{\mathbf{A}}(\alpha)$ is performed with L-BFGS-B optimizer [22]. In the following, we will work with the optimal vector α_ℓ^* , which is the approximation of α_{MAP} obtained at the end of the algorithm.

2.3.2 Confidence in the estimation.

As it stands, there is no guarantee that the obtained α_ℓ^* is close to the true α_{MAP} . More precisely, the goal is for the a posteriori pdf of α_ℓ^* to be close to the maximum a posteriori density across all $\alpha \in \mathcal{A}$. As detailed in Appendix A, with a statistical test, we then propose a confidence level $\gamma(\alpha)$ associated with $p(\alpha | \mathbf{y}_{1,\text{obs}}) < \beta p(\alpha_\ell^* | \mathbf{y}_{1,\text{obs}})$ for a given α , where β represents an acceptable margin of error this estimation, set by the user. For example, in the application, $\beta = 1.05$ is used, see Section 3.5, corresponding

to a tolerance of 5% on the a posteriori density. This confidence level will be computed for $\alpha \in \mathcal{A}$, as illustrated in Figure F.7b. A threshold ζ can be introduced, to ensure that $\forall \alpha \in \mathcal{A}, \gamma(\alpha) \geq \zeta$, with for instance $\zeta = 0.95$. To estimate these confidence levels and similarly to the approach in Section 2.4, we use $\hat{P}_L^{\alpha_\ell^*}(\mathbf{y}_{1,\text{obs}} | \alpha)$ as the estimator of $p(\mathbf{y}_{1,\text{obs}} | \alpha)$. More precisely, for this specific study, a number L' of samples is considered, with L' very large, to work with $\hat{P}_{L'}^{\alpha_\ell^*}(\mathbf{y}_{1,\text{obs}} | \alpha)$ and investigate the convergence, when L' goes to $+\infty$, of

$$\begin{aligned} & \hat{P}_{L'}^{\alpha_\ell^*}(\mathbf{y}_{1,\text{obs}} | \alpha) p_{\mathbf{A}}(\alpha) - \beta \hat{P}_{L'}^{\alpha_\ell^*}(\mathbf{y}_{1,\text{obs}} | \alpha_\ell^*) p_{\mathbf{A}}(\alpha_\ell^*) \\ &= \frac{1}{L'} \sum_{k=1}^{L'} \left(p(\mathbf{y}_{1,\text{obs}} | \Lambda'_k) \frac{p_{\mathbf{A}}(\Lambda'_k | \alpha) p_{\mathbf{A}}(\alpha) - \beta p_{\mathbf{A}}(\Lambda'_k | \alpha_\ell^*) p_{\mathbf{A}}(\alpha_\ell^*)}{p_{\mathbf{A}}(\Lambda'_k | \alpha_\ell^*)} \right), \end{aligned} \quad (8)$$

with $(\Lambda'_k)_{k=1}^{L'}$ i.i.d. with pdf $p_{\Lambda}(\cdot | \alpha_\ell^*)$.

We introduce the estimator

$$\begin{aligned} s_{L'}(\alpha)^2 &= \frac{1}{L' - 1} \sum_{k=1}^{L'} \left(p(\mathbf{y}_{1,\text{obs}} | \Lambda'_k) \frac{p_{\mathbf{A}}(\Lambda'_k | \alpha) p_{\mathbf{A}}(\alpha) - \beta p_{\mathbf{A}}(\Lambda'_k | \alpha_\ell^*) p_{\mathbf{A}}(\alpha_\ell^*)}{p_{\mathbf{A}}(\Lambda'_k | \alpha_\ell^*)} - \right. \\ & \quad \left. \left(\hat{P}_{L'}^{\alpha_\ell^*}(\mathbf{y}_{1,\text{obs}} | \alpha) p_{\mathbf{A}}(\alpha) - \beta \hat{P}_{L'}^{\alpha_\ell^*}(\mathbf{y}_{1,\text{obs}} | \alpha_\ell^*) p_{\mathbf{A}}(\alpha_\ell^*) \right) \right)^2. \end{aligned}$$

As detailed in Appendix A, with the Central Limit Theorem, we have the following asymptotic confidence level:

$$\gamma(\alpha) = \Phi \left(\frac{\sqrt{L'} \left(\beta \hat{P}_{L'}^{\alpha_\ell^*}(\mathbf{y}_{1,\text{obs}} | \alpha_\ell^*) p_{\mathbf{A}}(\alpha_\ell^*) - \hat{P}_{L'}^{\alpha_\ell^*}(\mathbf{y}_{1,\text{obs}} | \alpha) p_{\mathbf{A}}(\alpha) \right)}{s_{L'}(\alpha)} \right), \quad (9)$$

where Φ is the cumulative distribution function (cdf) of a Gaussian distribution with mean 0 and variance 1, and $s_{L'}(\alpha)$, $\hat{P}_{L'}^{\alpha_\ell^*}(\mathbf{y}_{1,\text{obs}} | \alpha_\ell^*)$ and $\hat{P}_{L'}^{\alpha_\ell^*}(\mathbf{y}_{1,\text{obs}} | \alpha)$ are the obtained realizations of the associated estimators.

2.4 Sampling from the posterior distribution of \mathbf{A}

Instead of working only with α_{MAP} as in the plug-in strategy, we can conduct a full-Bayesian strategy and work with the entire posterior distribution $p(\alpha | \mathbf{y}_{1,\text{obs}})$ estimated by

$$\hat{P}_L^{\alpha_\ell^*}(\alpha | \mathbf{y}_{1,\text{obs}}) = \frac{\hat{P}_L^{\alpha_\ell^*}(\mathbf{y}_{1,\text{obs}} | \alpha) p_{\mathbf{A}}(\alpha)}{\int_{\mathcal{A}} \hat{P}_L^{\alpha_\ell^*}(\mathbf{y}_{1,\text{obs}} | \alpha') p_{\mathbf{A}}(\alpha') d\alpha'}. \quad (10)$$

The method is summarized in Algorithm 2. Note that since $\|\alpha_\ell^* - \alpha_{\ell-1}^*\| \leq \tau$ with small τ , in practice $\hat{P}_L^{\alpha_{\ell-1}^*}(\alpha | \mathbf{y}_{1,\text{obs}})$, obtained from Algorithm 1 can be used to estimate $p(\alpha | \mathbf{y}_{1,\text{obs}})$. Therefore, no additional call to the simulator is required compared to the plug-in method. To simplify the notations and ensure everything depends only on α_ℓ^* , the method is presented with $\hat{P}_L^{\alpha_\ell^*}(\alpha | \mathbf{y}_{1,\text{obs}})$ as the estimator.

We have

$$\mathbb{E}(\Psi(Y_t(\mathbf{x}_0)) | \mathbf{y}_{1,\text{obs}}) = \int_{\mathcal{A}} \mathbb{E}(\Psi(Y_t(\mathbf{x}_0)) | \alpha, \mathbf{y}_{1,\text{obs}}) p(\alpha | \mathbf{y}_{1,\text{obs}}) d\alpha. \quad (11)$$

Appendix C shows that under additional assumptions on $\lambda \mapsto p(\mathbf{y}_{1,\text{obs}} | \lambda)$, $p_{\Lambda}(\cdot | \alpha)$ and $p_{\Lambda}(\lambda | \cdot)$, $\int_{\mathcal{A}} \mathbb{E}(\Psi(Y_t(\mathbf{x}_0)) | \alpha, \mathbf{y}_{1,\text{obs}}) \hat{P}_L^{\alpha_\ell^*}(\alpha | \mathbf{y}_{1,\text{obs}}) d\alpha$ is a consistent estimator of $\mathbb{E}(\Psi(Y_t(\mathbf{x}_0)) | \mathbf{y}_{1,\text{obs}})$.

Therefore, with MCMC methods, we sample $(\mathbf{A}_i)_{i=1}^N$ with pdf proportional to $\hat{P}_L^{\alpha_\ell^*}(\mathbf{y}_{1,\text{obs}}|\cdot)p_{\mathbf{A}}$ and investigate

$$\tilde{\mathbb{E}}_{N}^{\alpha_\ell^*}(\psi(Y_t(\mathbf{x}_0))) = \frac{1}{N} \sum_{i=1}^N \mathbb{E}(\psi(Y_t(\mathbf{x}_0)) \mid \mathbf{A}_i, \mathbf{y}_{1,\text{obs}}), \quad (12)$$

that approximates $\mathbb{E}(\psi(Y_t(\mathbf{x}_0)) \mid \mathbf{y}_{1,\text{obs}})$, but is not directly an estimator of $\mathbb{E}(\psi(Y_t(\mathbf{x}_0)) \mid \mathbf{y}_{1,\text{obs}})$, as $\mathbb{E}(\psi(Y_t(\mathbf{x}_0)) \mid \mathbf{A}_i, \mathbf{y}_{1,\text{obs}})$ is unknown.

Then $\mathbb{E}(\psi(Y_t(\mathbf{x}_0)) \mid \mathbf{A}_i, \mathbf{y}_{1,\text{obs}})$ needs to be estimated. As explained in Section 2.2, importance sampling estimation can be employed to reduce the computation cost. Indeed, from Equation (3), we have $\forall \alpha$ s.t. $\text{supp}(p_{\Lambda}(\cdot \mid \alpha)) \subset \text{supp}(p_{\Lambda}(\cdot \mid \alpha_\ell^*))$,

$$\mathbb{E}(\psi(Y_t(\mathbf{x}_0)) \mid \alpha, \mathbf{y}_{1,\text{obs}}) = \frac{\int_{\mathbb{R}^q} \psi(f_t(\mathbf{x}_0, \lambda)) p(\mathbf{y}_{1,\text{obs}} \mid \lambda) \frac{p_{\Lambda}(\lambda \mid \alpha)}{p_{\Lambda}(\lambda \mid \alpha_\ell^*)} p_{\Lambda}(\lambda \mid \alpha_\ell^*) d\lambda}{\int_{\mathbb{R}^q} p(\mathbf{y}_{1,\text{obs}} \mid \lambda) \frac{p_{\Lambda}(\lambda \mid \alpha)}{p_{\Lambda}(\lambda \mid \alpha_\ell^*)} p_{\Lambda}(\lambda \mid \alpha_\ell^*) d\lambda}. \quad (13)$$

It gives a full-Bayesian estimator of $\mathbb{E}(\psi(Y_t(\mathbf{x}_0)) \mid \mathbf{y}_{1,\text{obs}})$:

$$\hat{E}_{N,M}^{\alpha_\ell^*}(\psi(Y_t(\mathbf{x}_0))) = \frac{1}{N} \sum_{i=1}^N \frac{\sum_{k=1}^M \psi(f_t(\mathbf{x}_0, \mathbf{\Lambda}_k)) \frac{p_{\Lambda}(\mathbf{\Lambda}_k \mid \mathbf{A}_i)}{p_{\Lambda}(\mathbf{\Lambda}_k \mid \alpha_\ell^*)}}{\sum_{k=1}^M \frac{p_{\Lambda}(\mathbf{\Lambda}_k \mid \mathbf{A}_i)}{p_{\Lambda}(\mathbf{\Lambda}_k \mid \alpha_\ell^*)}}, \quad (14)$$

with $(\mathbf{A}_i)_{i=1}^N$ sampled with pdf proportional to $\hat{P}_L^{\alpha_\ell^*}(\mathbf{y}_{1,\text{obs}} \mid \alpha)p_{\mathbf{A}}(\alpha)$ and $(\mathbf{\Lambda}_k)_{k=1}^M$ sampled with pdf proportional to $p(\mathbf{y}_{1,\text{obs}} \mid \lambda)p_{\Lambda}(\lambda \mid \alpha_\ell^*)$. To ensure for all \mathbf{A}_i , the inclusion $\text{supp}(p_{\Lambda}(\cdot \mid \mathbf{A}_i)) \subset \text{supp}(p_{\Lambda}(\cdot \mid \alpha_\ell^*))$, $\sum_{k=1}^M \frac{p_{\Lambda}(\mathbf{\Lambda}_k \mid \mathbf{A}_i)}{p_{\Lambda}(\mathbf{\Lambda}_k \mid \alpha_\ell^*)} > 0$, and the consistency of the estimators (see Appendix C and Appendix D), in the following we impose

$$\exists \mathcal{K} \text{ compact set, } \forall \alpha \in \mathcal{A}, \text{supp}(p_{\Lambda}(\cdot \mid \alpha)) = \mathcal{K}. \quad (15)$$

Algorithm 2: Full-Bayesian estimation of $\mathbb{E}(\psi(Y_t(\mathbf{x}_0)) \mid \mathbf{y}_{1,\text{obs}})$.

Input: α_ℓ^*

Sample $(\mathbf{\Lambda}'_k)_{k=1}^L$ i.i.d. with pdf $p_{\Lambda}(\cdot \mid \alpha_\ell^*)$.

Sample $(\mathbf{A}_i)_{i=1}^N$ with pdf $\propto \hat{P}_L^{\alpha_\ell^*}(\mathbf{y}_{1,\text{obs}}|\cdot)p_{\mathbf{A}}$ by MCMC, with $\hat{P}_L^{\alpha_\ell^*}(\mathbf{y}_{1,\text{obs}}|\cdot)$ given by Equation (7).

Sample $(\mathbf{\Lambda}_k)_{k=1}^M$ with pdf $\propto p(\mathbf{y}_{1,\text{obs}} \mid \lambda)p_{\Lambda}(\lambda \mid \alpha_\ell^*)$ by MCMC.

Compute $\hat{E}_{N,M}^{\alpha_\ell^*}(\psi(Y_t(\mathbf{x}_0))) = \frac{1}{N} \sum_{i=1}^N \frac{\sum_{k=1}^M \psi(f_t(\mathbf{x}_0, \mathbf{\Lambda}_k)) \frac{p_{\Lambda}(\mathbf{\Lambda}_k \mid \mathbf{A}_i)}{p_{\Lambda}(\mathbf{\Lambda}_k \mid \alpha_\ell^*)}}{\sum_{k=1}^M \frac{p_{\Lambda}(\mathbf{\Lambda}_k \mid \mathbf{A}_i)}{p_{\Lambda}(\mathbf{\Lambda}_k \mid \alpha_\ell^*)}}$

If we consider $N = 1$ and $p_{\mathbf{A}} = \delta_{\alpha_\ell^*}$ in Equation (14), and $p_{\Lambda} = p_{\Lambda}(\cdot \mid \alpha_\ell^*)$ in Equation (4), then $\hat{E}_{N,M}^{\alpha_\ell^*}(\psi(Y_t(\mathbf{x}_0)))$ becomes equivalent to $\hat{E}_M(\psi(Y_t(\mathbf{x}_0)))$. The full-Bayesian estimator is a generalization of the estimator of Equation (4). Consequently, all equations related to $\hat{E}_{N,M}^{\alpha_\ell^*}(\psi(Y_t(\mathbf{x}_0)))$ in the following remain valid for $\hat{E}_M(\psi(Y_t(\mathbf{x}_0)))$.

More generally, we will denote

$$\hat{E}_{N,M}^{\alpha_\ell^*}(h(\mathbf{\Lambda})) = \frac{1}{N} \sum_{i=1}^N \frac{\sum_{k=1}^M h(\mathbf{\Lambda}_k) \frac{p_{\Lambda}(\mathbf{\Lambda}_k \mid \mathbf{A}_i)}{p_{\Lambda}(\mathbf{\Lambda}_k \mid \alpha_\ell^*)}}{\sum_{k=1}^M \frac{p_{\Lambda}(\mathbf{\Lambda}_k \mid \mathbf{A}_i)}{p_{\Lambda}(\mathbf{\Lambda}_k \mid \alpha_\ell^*)}}, \quad (16)$$

for every h function of $\mathbf{\Lambda}$ bounded and continuous on \mathcal{K} , with $(\mathbf{A}_i)_{i=1}^N$ sampled with pdf proportional to $\hat{P}_L^{\alpha_\ell^*}(\mathbf{y}_{1,\text{obs}} \mid \alpha)p_{\mathbf{A}}(\alpha)$ and $(\mathbf{\Lambda}_k)_{k=1}^M$ sampled with pdf proportional to $p(\mathbf{y}_{1,\text{obs}} \mid \lambda)p_{\Lambda}(\lambda \mid \alpha_\ell^*)$. It is the full-Bayesian estimator of $\mathbb{E}(h(\mathbf{\Lambda}) \mid \mathbf{y}_{1,\text{obs}})$ and it will be used with different h functions. From Appendix C and Appendix D, we have:

- $\int_{\mathcal{A}} \mathbb{E}(h(\Lambda) \mid \alpha, \mathbf{y}_{1,\text{obs}}) \hat{P}_L^{\alpha_\ell^*}(\alpha \mid \mathbf{y}_{1,\text{obs}}) d\alpha$ is a consistent estimator of $\mathbb{E}(h(\Lambda) \mid \mathbf{y}_{1,\text{obs}})$.
- Given $\hat{P}_L^{\alpha_\ell^*}(\alpha \mid \mathbf{y}_{1,\text{obs}}) = \hat{p}_L^{\alpha_\ell^*}(\alpha \mid \mathbf{y}_{1,\text{obs}})$, $\hat{E}_{N,M}^{\alpha_\ell^*}(h(\Lambda))$ is a consistent estimator of $\int_{\mathcal{A}} \mathbb{E}(h(\Lambda) \mid \alpha, \mathbf{y}_{1,\text{obs}}) \hat{p}_L^{\alpha_\ell^*}(\alpha \mid \mathbf{y}_{1,\text{obs}}) d\alpha$.

2.5 Surrogate modeling

In all of the above, we considered that we can perform runs of the simulator $f(\mathbf{x}, \lambda)$ to compute the estimators $\hat{E}_M(\psi(Y_t(\mathbf{x}_0)))$, $\hat{P}_L(\mathbf{y}_{1,\text{obs}} \mid \alpha)$ or $\hat{E}_{N,M}^{\alpha_\ell^*}(\psi(Y_t(\mathbf{x}_0)))$. It is important to note that in the approach presented here, the computation of the likelihood $p(\mathbf{y}_{1,\text{obs}} \mid \lambda) = p_E(\mathbf{y}_{1,\text{obs}} - (f_1(\mathbf{x}_j, \lambda))_{j=1}^n)$ requires n runs for a single λ . It leads to the following numbers of calls to the simulator:

- $L \times n \times \ell$ runs for the estimation of α_{MAP} , where ℓ is the number of iterations before convergence of Algorithm 1.
- $L \times n + M \times (n + 1)$ runs for the estimation of $\hat{E}_{N,M}^{\alpha_\ell^*}(\psi(Y_t(\mathbf{x}_0)))$. $n + 1$ comes from the fact that simulations must be run at $(\mathbf{x}_j)_{j=1}^n$ and at the new point \mathbf{x}_0 . If $\hat{p}_L^{\alpha_\ell^*}(\alpha \mid \mathbf{y}_{1,\text{obs}})$ is used at the likelihood approximation, then only $M \times (n + 1)$ runs are needed.

In practice, these computations are not feasible when the physical simulations are costly (for instance, several hours long each) and then surrogate models are required. First, surrogate models are required for the approximation of $(f_1(\mathbf{x}_j, \lambda))_{j=1}^n$ to compute the likelihood $p(\mathbf{y}_{1,\text{obs}} \mid \lambda) = p_E(\mathbf{y}_{1,\text{obs}} - (f_1(\mathbf{x}_j, \lambda))_{j=1}^n)$ for the MCMC sampling in the posterior distribution of Λ and the investigation of α_ℓ^* (see Algorithm 1). Additionally, a surrogate model is needed for $f_t(\mathbf{x}_0, \lambda)$ to compute the prediction estimator at the new point \mathbf{x}_0 for the unobserved output f_t . Therefore, for $\mathbf{x} \in \mathbb{X} \cup \{\mathbf{x}_0\}$ and $1 \leq t \leq T$, we propose to build a surrogate model for $f_{t,\mathbf{x}}: \lambda \rightarrow f_t(\mathbf{x}, \lambda)$.

Gaussian processes (GP) are used here as a surrogate model as they make it possible to quantify the uncertainties, as presented in [23]. Let us assume that $f_{t,\mathbf{x}}$ is a realization of a Gaussian process $Z_{t,\mathbf{x}}(\lambda)$ with prior mean $\mu_{t,\mathbf{x}}(\lambda)$ and prior covariance kernel $k_{t,\mathbf{x}}(\lambda, \lambda')$. $Z_{t,\mathbf{x}}$ and $Z_{t',\mathbf{x}'}$ are considered independent if $(t, \mathbf{x}) \neq (t', \mathbf{x}')$. The kernel models the correlation structure between $f_{t,\mathbf{x}}(\lambda)$ and $f_{t,\mathbf{x}}(\lambda')$. In our study, the stationary Matérn 5/2 kernel, see [24], is used. This choice of independency between the surrogate models implies that the Gaussian process used for the prediction at \mathbf{x}_0 is independent of the processes associated with the observations points \mathbf{x}_j .

We consider a design of experiments $\mathbb{L}_{\text{train}} = (\lambda_1, \dots, \lambda_{n_{\text{train}}})$ and the observations $Z_{t,\mathbf{x}}^{\text{train}} = (f_{t,\mathbf{x}}(\lambda_i))_{i \in I_{\text{train}}}$ with $I_{\text{train}} = \{1, \dots, n_{\text{train}}\}$. $f_{t,\mathbf{x}}$ can be approximated using the distribution of $Z_{t,\mathbf{x}}(\lambda) \mid Z(\mathbb{L}_{\text{train}}) = Z_{t,\mathbf{x}}^{\text{train}}$, which is a Gaussian process with the following mean and covariance:

$$\begin{cases} \hat{f}_t(\mathbf{x}, \lambda) = \mu_{t,\mathbf{x}}(\lambda) + k_{t,\mathbf{x}}(\lambda, \mathbb{L}_{\text{train}}) k_{t,\mathbf{x}}(\mathbb{L}_{\text{train}}, \mathbb{L}_{\text{train}})^{-1} (Z_{t,\mathbf{x}}^{\text{train}} - \mu_{t,\mathbf{x}}(\mathbb{L}_{\text{train}})) \\ c_t(\mathbf{x}, \lambda, \lambda') = k_{t,\mathbf{x}}(\lambda, \lambda') - k_{t,\mathbf{x}}(\lambda, \mathbb{L}_{\text{train}}) k_{t,\mathbf{x}}(\mathbb{L}_{\text{train}}, \mathbb{L}_{\text{train}})^{-1} k_{t,\mathbf{x}}(\lambda', \mathbb{L}_{\text{train}})^T \end{cases},$$

where $k(\mathbb{L}_{\text{train}}, \mathbb{L}_{\text{train}}) = [k_{t,\mathbf{x}}(\lambda_i, \lambda_j)]_{i,j \in I_{\text{train}}}$ is the covariance matrix and $k_{t,\mathbf{x}}(\lambda, \mathbb{L}_{\text{train}}) = [k_{t,\mathbf{x}}(\lambda, \lambda_i)]_{i \in I_{\text{train}}}$.

The variance is denoted $v_t(\mathbf{x}, \lambda) = c_t(\mathbf{x}, \lambda, \lambda)$. The model presented in Equation (2) then becomes:

$$\begin{cases} Y_t(\mathbf{x}) = \hat{f}_t(\mathbf{x}, \Lambda) + \sqrt{v_t(\mathbf{x}, \Lambda)} E^f(\mathbf{x}), & 1 \leq t \leq T, \mathbf{x} \in \mathcal{X} \\ Y_{1,\text{obs},j} = Y_1(\mathbf{x}_j) + E_j, & 1 \leq j \leq n \end{cases}, \quad (17)$$

with $E^f(\mathbf{x}) \sim \mathcal{N}(0, 1)$, $E^f(\mathbf{x}) \perp E^f(\mathbf{x}')$ if $\mathbf{x} \neq \mathbf{x}'$, and $\mathbf{E} = (E_j)_{j=1}^n$ of pdf p_E .

The pdf of the likelihood of λ becomes $p_{E^{\text{tot}}}(\lambda) \left((y_{1,\text{obs},j} - \hat{f}_1(\mathbf{x}_j, \lambda))_{j=1}^n \right)$ with

$$E^{\text{tot}}(\lambda) = \left(E_j + \sqrt{v_1(\mathbf{x}_j, \lambda)} E^f(\mathbf{x}_j) \right)_{j=1}^n. \quad (18)$$

Particularly, in our study we consider that p_E is the pdf of a Gaussian white noise vector, i.e. $E \sim \mathcal{N}(0, \sigma_\epsilon^2 I)$. This gives $E^{\text{tot}}(\lambda) \sim \mathcal{N}\left(0, \sigma_\epsilon^2 I + \text{diag}\left(v_1(\mathbf{x}_j, \lambda)\right)_{j=1}^n\right)$, and the estimators of the prediction mean and variance (from the law of total variance, see [25]) are

$$\begin{aligned} \hat{E}_{N,M}^{\alpha_\epsilon^*} \left(Y_t(\mathbf{x}_0) \right) &= \hat{E}_{N,M}^{\alpha_\epsilon^*} \left(\hat{f}_t(\mathbf{x}_0, \Lambda) \right) \\ \hat{E}_{N,M}^{\alpha_\epsilon^*} \left(Y_t(\mathbf{x}_0)^2 \right) - \hat{E}_{N,M}^{\alpha_\epsilon^*} \left(Y_t(\mathbf{x}_0) \right)^2 &= \\ \hat{E}_{N,M}^{\alpha_\epsilon^*} \left(\hat{f}_t(\mathbf{x}_0, \Lambda)^2 + v_t(\mathbf{x}_0, \Lambda) \right) - \hat{E}_{N,M}^{\alpha_\epsilon^*} \left(\hat{f}_t(\mathbf{x}_0, \Lambda) \right)^2 & \end{aligned} \quad (19)$$

3. APPLICATION

The previously introduced methods are tested on an application case well-suited for calibration with unobserved outputs, as presented here.

3.1 Case description

The test case considered here was developed by Rémi Chauvin from CEA DAM, and models the Taylor cylinder impact test [26], as illustrated in Figure 1. More precisely, it models the impact of a cylinder with length ℓ_0 , radius r_0 , launched at velocity v_0 against a rigid wall. This computer code requires 4 physical parameters associated with the Mie-Grüneisen equation of state [27] that are unknown and need to be calibrated. These parameters are ρ_0 the initial density of the cylinder, C_0 the bulk speed of sound, Γ_0 the Grüneisen coefficient at the reference state and S the Hugoniot slope parameter. In addition to these parameters to be calibrated, two additional variables Y_0 and Y_M can be taken into account to represent the model error. They are related to Ludwik's equation which describes the electroplastic deformation process: $\sigma = Y_0 + Y_M \epsilon_p^{n_0}$, where σ is the stress, Y_0 the yield stress, Y_M the strength index, ϵ_p the plastic strain and n_0 is the strain hardening index [28]. Thus, in our study we have

- 3 control variables $\mathbf{x} = (\ell_0, r_0, v_0)$
- $p = 4$ parameters to calibrate ρ_0, C_0, Γ_0, S
- $q - p = 2$ additional parameters Y_0 and Y_M .

This computer code is interesting in our context because it produces 3 outputs:

- The length difference $\ell_f - \ell_0$ after impact
- The final radius r_f
- The maximum strain over time $\epsilon_{\max} = \max \epsilon_p$

Therefore, we will consider 3 different transpositions: the first case where we have observations of $\ell_f - \ell_0$ only, the second with observations of r_f only, and finally the third with observations of ϵ_{\max} only. All input variables are constrained by predefined bounds, beyond which the simulation is not feasible. In the following, to simplify, they are all considered as normalized between 0 and 1.

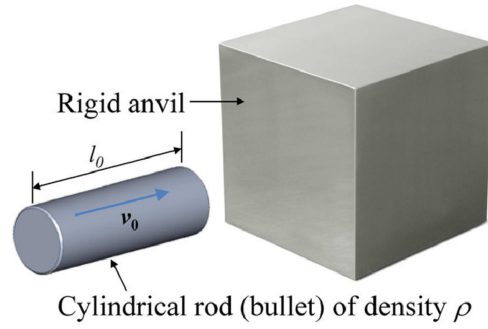


Figure 1: Diagram describing the Taylor cylinder impact test.

3.2 Model error

Unfortunately, there was no real experimental data to use in our study. However, one can easily build virtual measurements and integrate a custom model error to work in the previously described context.

For a given triplet $\mathbf{x} = (\ell_0, r_0, v_0)$, we define $\omega(\mathbf{x}) = (\ell_0, r_0, v_0 + \Delta V)$, where ΔV is fixed to a constant in our work. For $1 \leq t \leq T$, the true value is introduced as $y_t(\mathbf{x}) = f_t(\omega(\mathbf{x}), \lambda_0)$ for a given $\lambda_0 \in \mathcal{L}$, leading to a model error as there is no specific value of λ that verifies that $\forall \mathbf{x} \in \mathcal{X}, f_t(\mathbf{x}, \lambda) = y_t(\mathbf{x})$. Then the protocol is the following:

- Select n points $\mathbb{X} = (\mathbf{x}_j)_{j=1}^n \in \mathcal{X}^n$ with Latin Hypercube Sampling [29],
- Compute $(y_t(\mathbf{x}_j))_{j=1}^n = (f_t(\omega(\mathbf{x}_j), \lambda_0))_{j=1}^n$,
- Add a realization $\mathcal{E} = (\mathcal{E}_j)_{j=1}^n$ of the vector $\mathbf{E} \sim \mathcal{N}(0, \sigma_\varepsilon^2 I)$ as the measurement error for the observed variable.

Finally it provides the vector of experimental data,

$$\mathbf{y}_{1,\text{obs}} = (y_1(\mathbf{x}_j) + \mathcal{E}_j)_{j=1}^n.$$

3.3 Performance metrics

Beyond the measurements of the first variable $\mathbf{y}_{1,\text{obs}} = (y_{1,\text{obs},j})_{j=1}^n = (y_1(\mathbf{x}_j) + \mathcal{E}_j)_{j=1}^n \in \mathbb{R}^n$, here we also have access to the true values $y_t(\mathbf{x}_j)$ for $1 \leq t \leq T, 1 \leq j \leq n$. This makes it possible to assess the performance of the method. A Leave-One-Out (LOO) approach is used, to predict $y_t(\mathbf{x}_{j'})$ for $1 \leq j' \leq n$ based on the noisy observations $\mathbf{y}_{1,\text{obs}}^{-j} = (y_1(\mathbf{x}_j) + \mathcal{E}_j)_{j=1, j \neq j'}^n$. Then, a specific α_ℓ^* is identified for every j , that will be denoted α_ℓ^{j*} . Performance metrics are introduced to validate the results.

3.3.1 Prediction error.

The first criterion that matters in our situation is that the mean prediction is close to the true value. Thus, for a given $1 \leq t \leq T$ and for every $1 \leq j \leq n$, we compute a vector of predictions $\left(\hat{e}_{N,M}^{\alpha_\ell^{j*}} \left(Y_t(\mathbf{x}_j) \right) \right)_{j=1}^n$ (with LOO prediction), and we compare it to the vector of true values $(y_t(\mathbf{x}_j))_{j=1}^n$, by introducing the root mean squared relative error (RMSRE, [30]):

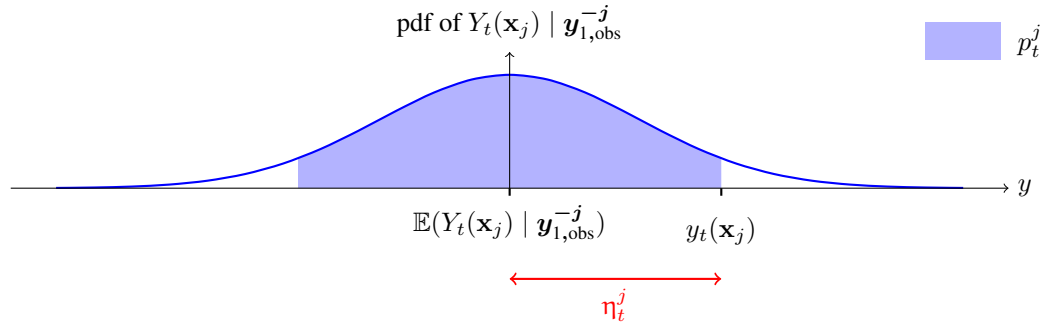


Figure 2: Illustration of the probability p_t^j represented by the shaded blue area under the curve. The blue curve is the pdf of $Y_t(\mathbf{x}_j) \mid \mathbf{y}_{1,\text{obs}}^{-j}$.

$$\delta_{t,N,M} = \sqrt{\frac{1}{n} \sum_{j=1}^n \left(\frac{|\hat{e}_{N,M}^{\alpha_t^{j*}}(Y_t(\mathbf{x}_j)) - y_t(\mathbf{x}_j)|}{y_t(\mathbf{x}_j)} \right)^2}. \quad (20)$$

This prediction error is a relevant metric but is not sufficient, as a small error is not necessarily associated with a validation of the probabilistic model.

3.3.2 Prediction interval.

As studied in [31], the width of prediction intervals is essential to validate the probabilistic model. Here, we investigate the smallest prediction interval that includes the true value. More precisely, for every $1 \leq j \leq n$, we investigate

$$p_t^j = \mathbb{P} \left(\left| Y_t(\mathbf{x}_j) - \mathbb{E}(Y_t(\mathbf{x}_j) \mid \mathbf{y}_{1,\text{obs}}^{-j}) \right| \leq \eta_t^j \mid \mathbf{y}_{1,\text{obs}}^{-j} \right), \quad (21)$$

with $\eta_t^j = |y_t(\mathbf{x}_j) - \mathbb{E}(Y_t(\mathbf{x}_j) \mid \mathbf{y}_{1,\text{obs}}^{-j})|$.

This probability p_t^j is computed based on the posterior distribution of $Y_t(\mathbf{x}_j) = f_t(\mathbf{x}_j, \mathbf{\Lambda}) = \hat{f}_t(\mathbf{x}_j, \mathbf{\Lambda}) + \sqrt{v_t(\mathbf{x}_j, \mathbf{\Lambda})} E^f(\mathbf{x}_j)$ given the LOO observations $\mathbf{y}_{1,\text{obs}}^{-j}$, and is the level of the smallest prediction interval that includes $y_t(\mathbf{x}_j)$, as illustrated in Figure 2. It can also be seen as the complementary probability of the p-value associated with the hypothesis $H_0 : Y_t(\mathbf{x}) = f_t(\mathbf{x}, \mathbf{\Lambda})$.

We have

$$\begin{aligned} p_t^j &= \mathbb{P} \left(\left| Y_t(\mathbf{x}_j) - \mathbb{E}(Y_t(\mathbf{x}_j) \mid \mathbf{y}_{1,\text{obs}}^{-j}) \right| \leq \eta_t^j \mid \mathbf{y}_{1,\text{obs}}^{-j} \right) \\ &= \mathbb{E} \left(\Phi \left(\frac{b_t^j - \hat{f}_t(\mathbf{x}_j, \mathbf{\Lambda})}{\sqrt{c_t(\mathbf{x}_j, \mathbf{\Lambda})}} \right) - \Phi \left(\frac{a_t^j - \hat{f}_t(\mathbf{x}_j, \mathbf{\Lambda})}{\sqrt{c_t(\mathbf{x}_j, \mathbf{\Lambda})}} \right) \mid \mathbf{y}_{1,\text{obs}}^{-j} \right), \end{aligned}$$

with $a_t^j = \mathbb{E}(Y_t(\mathbf{x}_j) \mid \mathbf{y}_{1,\text{obs}}^{-j}) - \eta_t^j$, $b_t^j = \mathbb{E}(Y_t(\mathbf{x}_j) \mid \mathbf{y}_{1,\text{obs}}^{-j}) + \eta_t^j$.

Then we work with the estimator

$$\hat{P}_{t,N,M}^j = \hat{E}_{N,M}^{\alpha_t^{j*}} \left(\Phi \left(\frac{\hat{B}_{t,N,M}^j - \hat{f}_t(\mathbf{x}_j, \mathbf{\Lambda})}{\sqrt{c_t(\mathbf{x}_j, \mathbf{\Lambda})}} \right) - \Phi \left(\frac{\hat{A}_{t,N,M}^j - \hat{f}_t(\mathbf{x}_j, \mathbf{\Lambda})}{\sqrt{c_t(\mathbf{x}_j, \mathbf{\Lambda})}} \right) \right), \quad (22)$$

with $\hat{A}_{t,N,M}^j = \hat{E}_{N,M}^{\alpha_t^{j*}}(Y_t(\mathbf{x}_j)) - |y_t(\mathbf{x}_j) - \hat{E}_{N,M}^{\alpha_t^{j*}}(Y_t(\mathbf{x}_j))|$ and $\hat{B}_{t,N,M}^j = \hat{E}_{N,M}^{\alpha_t^{j*}}(Y_t(\mathbf{x}_j)) + |y_t(\mathbf{x}_j) - \hat{E}_{N,M}^{\alpha_t^{j*}}(Y_t(\mathbf{x}_j))|$. As for $1 \leq t \leq T$, we obtain a vector of realizations $(\hat{p}_{t,N,M}^j)_{j=1}^n$, we will aggregate it and extract $\mathcal{Q}_{0.9}$ its 0.9 empirical quantile:

$$\hat{p}_{t,N,M}^{0,9} = \mathcal{Q}_{0.9} \left(\left[\hat{p}_{t,N,M}^j \right]_{j=1}^n \right). \quad (23)$$

3.4 Comparison of methods

To perform a comprehensive analysis of our method, we implement different approaches and compare the previously introduced performance metrics (see Section 3.3). All these approaches are summarized in Table 1.

	Formulation	Distribution
No error	$Y_t(\mathbf{x}) = f_t(\mathbf{x}, \Lambda)$ $\Lambda \in \mathbb{R}^p$	$p_{\Lambda}(\lambda) = 1_{[0,1]^p}$
Uniform error	$Y_t(\mathbf{x}) = f_t(\mathbf{x}, \Lambda)$ $\Lambda \in \mathbb{R}^q$	$p_{\Lambda}(\lambda) = 1_{[0,1]^q}$
Hierarchical MAP	$Y_t(\mathbf{x}) = f_t(\mathbf{x}, \Lambda)$ $\Lambda \in \mathbb{R}^q$	$p_{\Lambda}(\lambda \mid \alpha_{\ell}^*) =$ $1_{[0,1]^p}(\lambda_1, \dots, \lambda_p)$ $\times f_{\mathcal{N}_t}(\alpha_{\ell}^*, 0.45^2, 0, 1)(\lambda_{p+1}, \dots, \lambda_q)$
Hierarchical full Bayes	$Y_t(\mathbf{x}) = f_t(\mathbf{x}, \Lambda)$ $\Lambda \in \mathbb{R}^q$	$p_{\Lambda}(\lambda \mid \mathbf{A}) =$ $1_{[0,1]^p}(\lambda_1, \dots, \lambda_p)$ $\times f_{\mathcal{N}_t}(\mathbf{A}, 0.45^2, 0, 1)(\lambda_{p+1}, \dots, \lambda_q)$
Embedded discrepancy	$Y_t(\mathbf{x}) = f_t(\mathbf{x}, \Lambda^1 + \delta(\Lambda^2, \Xi))$ $\Lambda^1 \in \mathbb{R}^q, \Lambda^2 \in \mathbb{R}^q$	$\delta(\Lambda^2, \Xi) = \text{diag}(\Lambda^2 \Xi^T)$ $\Xi \sim \mathcal{U}([-1, 1]^q)$ $p_{(\Lambda^1, \Lambda^2)}(\lambda^1, \lambda^2) \propto$ $\prod_{i=1}^q 1_{\lambda_i^2 > 0} 1_{\lambda_i^1 - \lambda_i^2 > 0} 1_{\lambda_i^1 + \lambda_i^2 < 1}$

Table 1: Summary of all the methods investigated in our study.

The first approach is to consider no model error in our bayesian framework, and is called *No error*. We then consider $\lambda = (\rho_0, C_0, \Gamma_0, S) \in \mathcal{L}_{\text{cal}} \subset \mathbb{R}^p$ with a non-informative prior distribution $\mathcal{U}_{[0,1]^p}$. Then we can implement the method described in Section 2.1, and work with the estimator $\hat{E}_M(\psi(Y_t(\mathbf{x}_0)))$ with $p_{\Lambda} = 1_{[0,1]^p}$.

The second idea is to introduce the additionnal parameters Y_0 and Y_M to represent the model error, but without a hierarchical model. Indeed, we consider $\lambda = (\rho_0, C_0, \Gamma_0, S, Y_0, Y_M) \in \mathcal{L}_{\text{cal}} \times \mathcal{L}_{\text{err}} \subset \mathbb{R}^q$ and investigate $\hat{E}_M(\psi(Y_t(\mathbf{x}_0)))$ with $p_{\Lambda} = 1_{[0,1]^q}$. It is called *Uniform error*.

The third method, called *Hierarchical MAP*, includes the additionnal parameters Y_0 and Y_M with the hierarchical model using a plug-in strategy. It investigates α_{ℓ}^* as described in Section 2.3, and then studies

$\hat{E}_M(\psi(Y_t(\mathbf{x}_0)))$ with $p_{\Lambda}(\cdot | \alpha_{\ell}^*)$. In our work, we consider

$$p_{\Lambda}(\lambda | \alpha) = 1_{[0,1]^p}(\lambda_1, \dots, \lambda_p) \times f_{\mathcal{N}_t}(\alpha, 0.45^2, 0, 1)(\lambda_{p+1}, \dots, \lambda_q), \quad (24)$$

where $f_{\mathcal{N}_t}(\mu, \sigma^2, a, b)$ is the pdf of a Gaussian distribution with mean μ and standard deviation σ truncated between a and b . We can note that the standard deviation $\sigma = 0.45$ is chosen to investigate prior distributions that are exploratory enough.

The fourth method is the one described in Section 2.4, considering a model error with a hierarchical description but with a full-Bayesian approach, to compute the estimator $\hat{E}_{N,M}^{\alpha_{\ell}^*}(\psi(Y_t(\mathbf{x}_0)))$. We call it *Hierarchical full Bayes*. We consider the prior $p_{\Lambda} = p_{\Lambda}(\cdot | \alpha)$ described in Equation (24), and $p_{\mathbf{A}}$ the pdf of the uniform distribution $\mathcal{U}_{\mathcal{I}}(\alpha_{\ell}^*, \kappa)$, with $\mathcal{I}(\alpha_{\ell}^*, \kappa) = [(\alpha_{\ell}^*)_1 - \kappa, (\alpha_{\ell}^*)_1 + \kappa] \times \dots \times [(\alpha_{\ell}^*)_r - \kappa, (\alpha_{\ell}^*)_r + \kappa] \cap [-10, 10]^r$, and $\kappa \in \mathbb{R}$. The constant κ is introduced to prevent the investigation of zones with high fluctuations of $\frac{p_{\Lambda}(\Lambda_k | \alpha)}{p_{\Lambda}(\Lambda_k | \alpha_{\ell}^*)}$. We work with $\kappa = 4$ here. Note that this choice of prior $p_{\mathbf{A}}$ allows for negative values of α (or values higher than 1), that can concentrate $p_{\Lambda}(\cdot | \alpha)$ on a zone near 0 (or a zone near 1, respectively).

Finally, the last approach is the one presented in [13], called *Embedded discrepancy* here. Their work is particularly interesting in our context as they consider a model error that is embedded in the calibration parameters and then can be set up in our transposition situation, as detailed in Appendix E.

Every MCMC sampling is implemented with the package `pymcmcstat` [32], and the optimization of the hyperparameters for the Gaussian Process regression is performed with `pylibkriging` [33]. The number of observations is set to $n = 10$. $L = 10^4$ samples are considered to estimate α_{MAP} , while $M = 3000$ posterior samples of Λ and $N = 750$ samples of \mathbf{A} are generated to compute $\hat{E}_{N,M}^{\alpha_{\ell}^*}(\psi(Y_t(\mathbf{x}_0)))$. Note that $N < M$ as $\mathcal{A} \subset \mathbb{R}^2$ compared to $\mathcal{L} \subset \mathbb{R}^6$. $L' = 2 \times 10^4$ samples are used for the estimation of the confidence levels associated with $p(\alpha | \mathbf{y}_{1,\text{obs}}) < \beta p(\alpha_{\ell}^* | \mathbf{y}_{1,\text{obs}})$.

3.5 Numerical results

The methods are implemented on different designs $\mathbb{X} = (\mathbf{x}_j)_{j=1}^{10}$ for consistency. While only one design is presented here, the remaining results are provided in the Supplementary Material [34], and the conclusions remain consistent across all designs.

3.5.1 Results overview.

The results are shown in Figures 4, 5, 6 corresponding to observations of $\ell_f - \ell_0$, r_f and ϵ_{max} , respectively. For each figure, the first plot shows the mean and the standard deviation of the normalized posterior distribution $\frac{Y_t(\mathbf{x}_j) - y_t(\mathbf{x}_j)}{y_t(\mathbf{x}_j)} | \mathbf{y}_{1,\text{obs}}$ for each method and $1 \leq j \leq 10$, and compare it to the true values $y_t(\mathbf{x}_j)$ shifted to 0 represented with blue crosses for $1 \leq t \leq 3$. From these posterior distributions, the performance metrics are computed and displayed in the second plot. The RMSRE and $\hat{p}_{t,N,M}^{0,9}$ (both in %) are represented with the blue bar and the green bar, respectively.

The first notable observation is the performance gain associated with the inclusion of the additional two parameters Y_0 and Y_M , to represent the model error. Indeed, whether considering precision (low RMSRE) or model validation (low probability levels $\hat{p}_{t,N,M}^{0,9}$), the results are consistently better with these additional parameters than without them, for any method used to account for the model error. More specifically, regarding the model error, the two hierarchical approaches (the *Hierarchical MAP* and *Hierarchical full Bayes* methods) are almost identical and significantly improve the results compared to the uniform error approach. In fact, except for the transposition from $\ell_f - \ell_0$ to ϵ_{max} , the RMSRE is 1.5 to 5 times lower with the hierarchical approach. For this specific transposition, the probabilistic model is clearly validated with a probability $\hat{p}_{t,N,M}^{0,9} = 40\%$ for the hierarchical full Bayes method. Similarly, for all tested transpositions, the confidence interval levels are favorable with the hierarchical approach, with all probabilities $\hat{p}_{t,N,M}^{0,9}$ being below 95%.

The embedded discrepancy approach shows less favorable results compared to the hierarchical approach, with, for example, probabilities $\hat{p}_{t,N,M}$ exceeding 99.5% for transpositions based on r_f measurements.

To interpret these results, it is necessary to examine $p(\boldsymbol{\lambda} \mid \mathbf{y}_{1,\text{obs}})$ the pdf of the a posteriori distribution of $\boldsymbol{\lambda}$ for the different methods. Since a LOO scheme is applied, a distinct posterior sample $(\boldsymbol{\lambda}_k)_{k=1}^M$ (or $(\boldsymbol{\lambda}_k^1 + \boldsymbol{\lambda}_k^2 \boldsymbol{\xi}_r)_{r=1,\dots,R}$ for the *Embedded discrepancy*) is obtained for each \mathbf{x}_j and each method, except for the *Hierarchical MAP* and *Hierarchical full Bayes* methods, where the samples are identical, as discussed in Section 2.4. Figure 3 presents the marginal distributions of a posteriori samples obtained for predicting \mathbf{x}_{10} based on measurements of $\ell_f - \ell_0$, but similar results are observed when targeting another \mathbf{x}_j or with a different calibration variable.

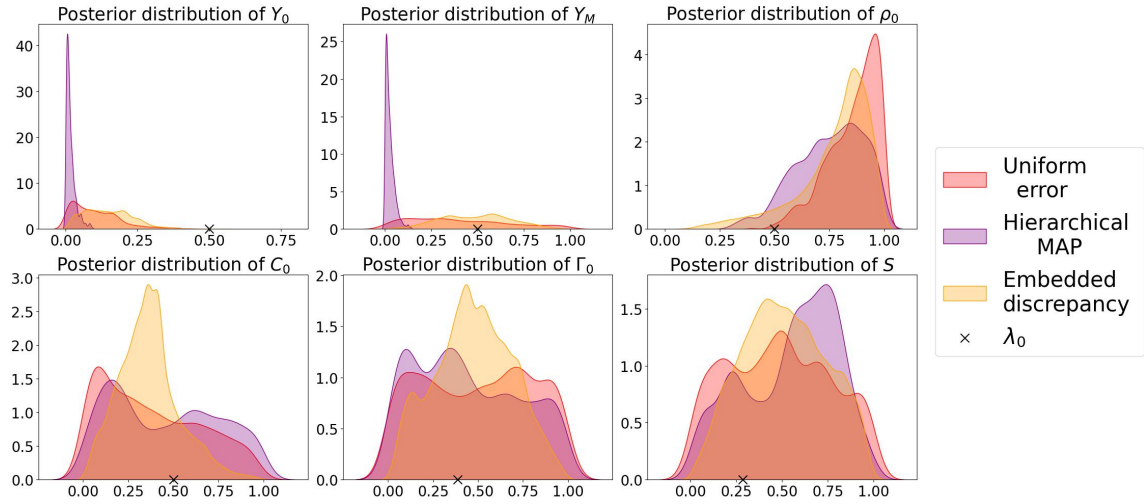


Figure 3: Distribution of each marginal of the a posteriori samples $(\boldsymbol{\lambda}_k)_{k=1}^M$ obtained with the *Uniform error* and the *Hierarchical MAP* strategies, and the samples $(\boldsymbol{\lambda}_k^1 + \boldsymbol{\lambda}_k^2 \boldsymbol{\xi}_r)_{r=1,\dots,R}$ for the *Embedded discrepancy*, for the prediction at \mathbf{x}_{10} from observations of $\ell_f - \ell_0$. The black cross is associated with $\boldsymbol{\lambda}_0$, the parameters used for the measurements acquisition.

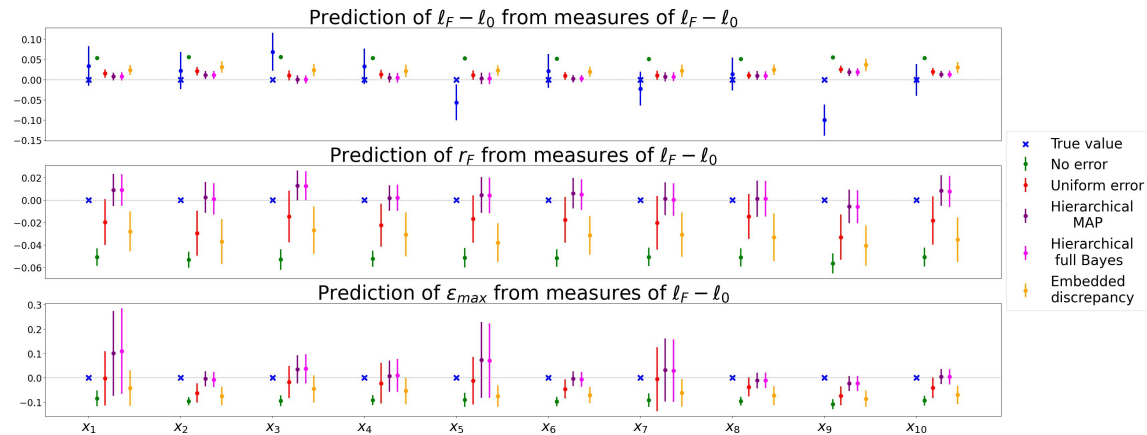
3.5.2 Analysis for the hierarchical model.

In Figure 3, it clearly appears that the hierarchical model completely drives the additional parameters Y_0 and Y_M to values near 0, which leads to better results. The influence of this approach is amplified by the fact that the observation noise is set high, with standard deviations of 0.9 for $\ell_f - \ell_0$ and r_f , and 0.3 for ϵ_{\max} (see Figures 4a, 5a, 6a). Indeed, the larger the noise variance, the less concentrated the likelihood of $\boldsymbol{\lambda}$, thereby increasing the influence of the prior. Appendix G shows the transposition results obtained with smaller observation noises.

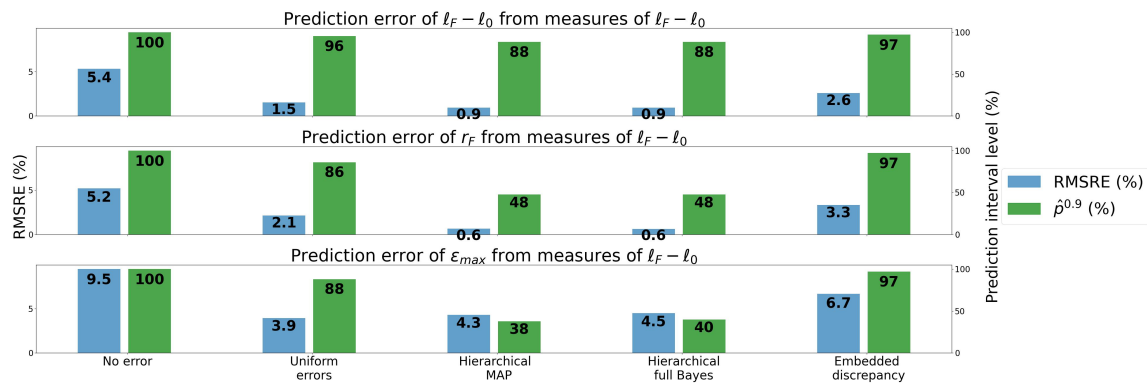
The almost identical results between *Hierarchical MAP* and *Hierarchical full Bayes* is explained by the posterior distribution $p(\boldsymbol{\alpha} \mid \mathbf{y}_{1,\text{obs}})$ that overall focuses on negative values of $\boldsymbol{\alpha}$ and then drives the normalized $\boldsymbol{\lambda}$ very close to 0, with very small difference compared to the identified $\boldsymbol{\alpha}_\ell^*$. Indeed, the prior $p_{\mathbf{A}}(\cdot \mid \boldsymbol{\alpha})$ is concentrated on zones near 0 for $\boldsymbol{\alpha} = \boldsymbol{\alpha}_\ell^*$ and for all the values $\boldsymbol{\alpha}$ that are sampled with $p(\boldsymbol{\alpha} \mid \mathbf{y}_{1,\text{obs}})$. Appendix F illustrates this posterior distribution for a specific \mathbf{x}_j and $y_1 = \epsilon_{\max}$ (see Figure F.7a), and shows that the asymptotic confidence levels $\gamma(\boldsymbol{\alpha})$ associated with $p(\mathbf{y}_{1,\text{obs}} \mid \boldsymbol{\alpha})p_{\mathbf{A}}(\boldsymbol{\alpha}) < 1.05p(\mathbf{y}_{1,\text{obs}} \mid \boldsymbol{\alpha}_\ell^*)p_{\mathbf{A}}(\boldsymbol{\alpha}_\ell^*)$ are promising, with $\forall \boldsymbol{\alpha}, \gamma(\boldsymbol{\alpha}) > 0.99$.

3.5.3 Analysis for the embedded discrepancy.

Regarding the performance of the *embedded discrepancy* approach, it is evident that the prediction error consistently occurs in the same direction: $\ell_f - \ell_0$ is overestimated, while r_f and ϵ_{\max} are underestimated. This can be attributed to the fact that, as is often the case in the presence of model error, the highest likelihoods of λ are located at the boundaries, particularly for Y_0 and ρ_0 (see Figure 3). The influence of these variables on the outputs can be seen as monotonic, as highlighted by linear regression: increasing Y_0 leads to an increase in $\ell_f - \ell_0$ but a decrease in r_f and ϵ_{\max} , and the opposite is true for ρ_0 . However, as expected, the *embedded discrepancy* approach is more exploratory in its sampling, considering a wider range of values for Y_0 and ρ_0 away from the boundary. This increases the predicted mean of $\ell_f - \ell_0$ and decreases it for r_f and ϵ_{\max} , since no sampling is possible beyond the boundary to balance this exploration.



(a) Mean and standard deviation of the normalized posterior distribution $\frac{Y_t(\mathbf{x}_j) - y_t(\mathbf{x}_j)}{y_t(\mathbf{x}_j)} \mid \mathbf{y}_{1,\text{obs}}^{-j}$, $1 \leq j \leq 10$, with $y_1 = \ell_f - \ell_0$, compared to the true values $y_t(\mathbf{x}_j)$ shifted to 0 shown as blue crosses for $1 \leq t \leq 3$. The normalized measurement of $\ell_f - \ell_0$ is indicated by the blue dot, with its standard deviation represented by the associated error bar.

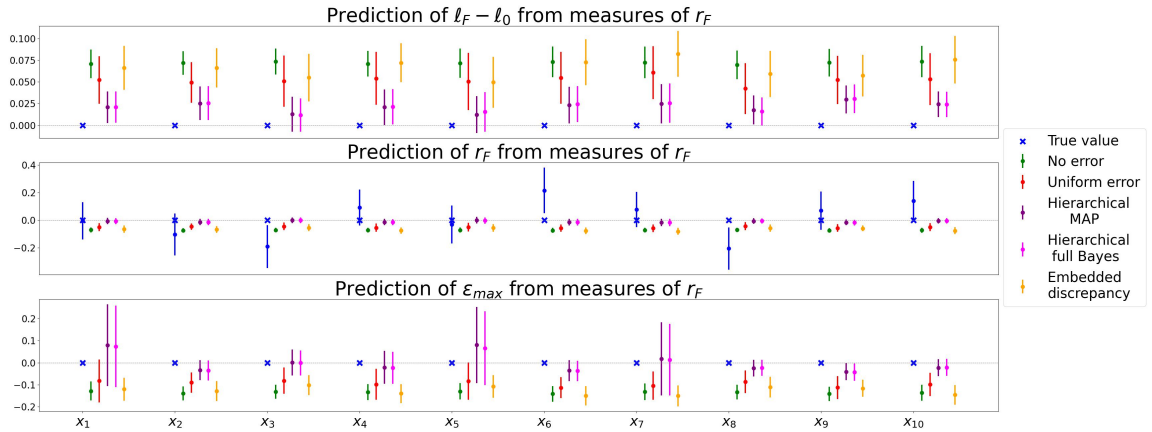


(b) Performance metrics from observations of $\ell_f - \ell_0$. The blue bar is the RMSRE in %, while the green bar represent $\hat{\rho}_{t,N,M}^{0.9}$ in %, the 0.9 quantile of the aggregated levels of the smallest prediction intervals.

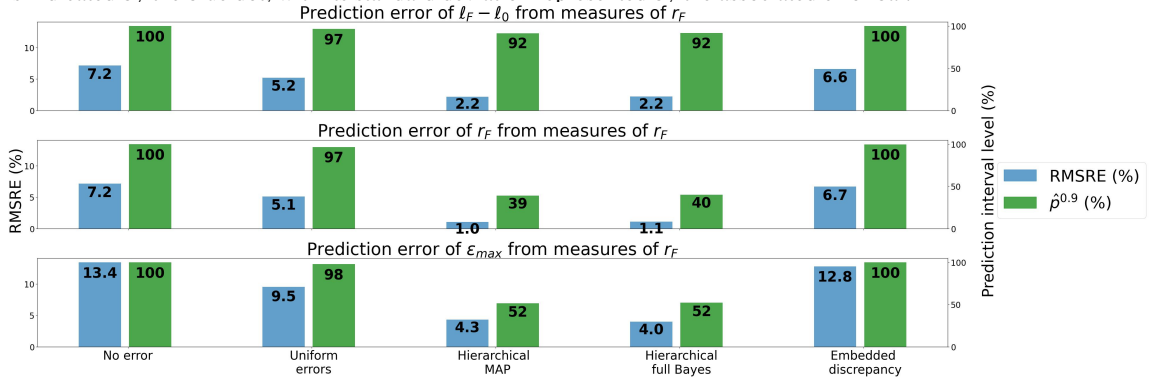
Figure 4: Prediction of the three outputs from observations of $\ell_f - \ell_0$.

4. SUMMARY AND PERSPECTIVES

This article addresses the transposition problem, which occurs when observed experimental data do not correspond directly to the data of interest. It specifically examines a scenario with multiple outputs, where



(a) Mean and standard deviation of the normalized posterior distribution $\frac{Y_t(\mathbf{x}_j) - y_t(\mathbf{x}_j)}{y_t(\mathbf{x}_j)} \mid \mathbf{y}_{1,\text{obs}}^{-j}$, $1 \leq j \leq 10$, with $y_1 = r_f$, compared to the true values $y_t(\mathbf{x}_j)$ shifted to 0 shown as blue crosses for $1 \leq t \leq 3$. The measurement of r_f is indicated by the blue dot, with its standard deviation represented by the associated error bar.

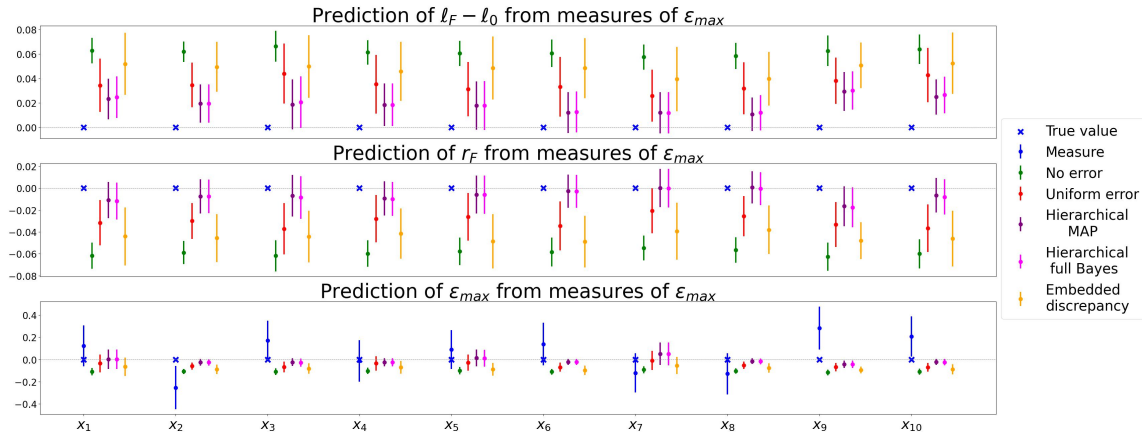


(b) Performance metrics from observations of r_f . The blue bar is the RMSRE in %, while the green bar represent $\hat{p}_{t,N,M}^{0.9}$ in %, the 0.9 quantile of the aggregated levels of the smallest prediction intervals.

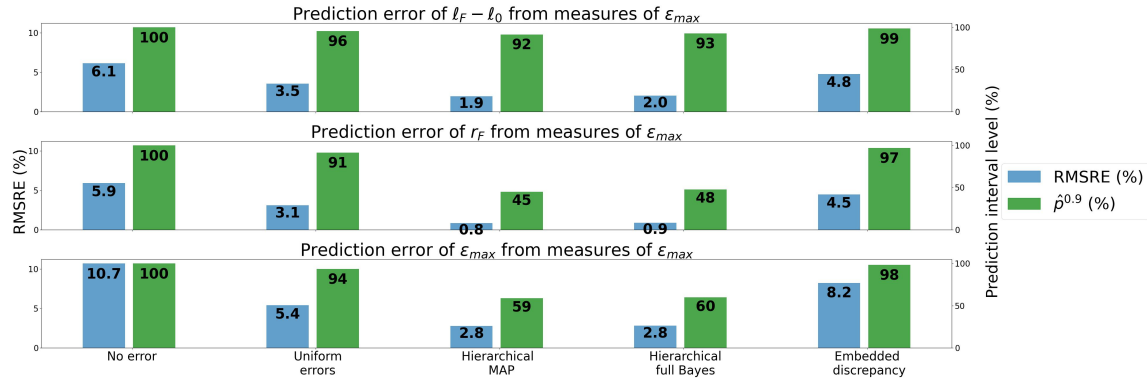
Figure 5: Prediction of the three outputs from observations of r_f

only one output is experimentally observed, while the goal is to predict all of them. The main idea is to propose a representation of the model error that is adapted to this situation, and thus needs to be embedded in the parameters Λ to establish a relationship between the observations and the unobserved outputs. Specifically, the inclusion of additional parameters in Λ , typically numerical ones that were not initially intended for calibration, is explored. These parameters are incorporated to account for model error through a hierarchical representation, directing this error into specific zones by introducing hyperparameters α for the prior distribution. The estimation of these hyperparameters is then conducted using Bayesian inference, either by identifying the maximum a posteriori α_{MAP} or by sampling from the posterior distribution, with an importance sampling scheme to significantly reduce the computational cost. This study is conducted in the context of expensive simulations, with Gaussian process regression as a surrogate model.

The application test case of the article models the Taylor cylinder impact test, which involves three outputs considered as observed variables one at a time, leading to three different sets of results. The performance of our method is compared to the approach proposed by [13], which introduces an *Embedded Discrepancy* method relevant to our scenario. It is important to keep in mind that the results of these Bayesian approaches are highly dependent on the specific application case.



(a) Mean and standard deviation of the normalized posterior distribution $\frac{Y_t(\mathbf{x}_j) - y_t(\mathbf{x}_j)}{y_t(\mathbf{x}_j)} \mid \mathbf{y}_{1,\text{obs}}^{-j}$, $1 \leq j \leq 10$, with $y_1 = \epsilon_{\max}$, compared to the true values $y_t(\mathbf{x}_j)$ shifted to 0 shown as blue crosses for $1 \leq t \leq 3$. The measurement of ϵ_{\max} is indicated by the blue dot, with its standard deviation represented by the associated error bar.



(b) Performance metrics from observations of ϵ_{\max} . The blue bar is the RMSRE in %, while the green bar represent $\hat{p}_{t,N,M}^{0.9}$ in %, the 0.9 quantile of the aggregated levels of the smallest prediction intervals.

Figure 6: Prediction of the three outputs from observations of ϵ_{\max} .

The results obtained here demonstrate a significant impact of the hierarchical model, in terms of low prediction error (RMRSE) or validation of the probabilistic models through the investigation of prediction intervals. This impact is somewhat reduced when a small noise measurement variance is considered, although the hierarchical approach remains well-suited. In contrast, the *Embedded Discrepancy* method from [13] performs less effectively in our context, partly due to the fact that the most likely values of Λ are located near the boundaries. Additionally, the Legendre-Uniform Polynomial Chaos (Legendre-Uniform PC) representation used in this study could be further modified to potentially enhance these results.

Although the study presented here is comprehensive, further developments should be considered. As explained in Section 3.5, the influence of the prior on Λ is reduced when the noise measurement variance is small, although the results of the hierarchical model remain promising in this situation, as shown in Appendix G. An in-depth study of the relationship between the impact of the hierarchical representation and the noise measurement could be valuable, potentially identifying a threshold on the noise variance below which the likelihood on Λ becomes too concentrated, resulting in a non-influential prior.

Another important aspect of the work is the surrogate model implemented with Gaussian process regression. Here, a different Gaussian process is considered for every $\mathbf{x} \in \mathcal{X}$ and $1 \leq t \leq T$, and they are

all considered independent. This allows to tackle situations where the \mathbf{x}_j are categorical values for instance. However, other implementations are possible, considering a Gaussian process $Z_t(\mathbf{x}, \boldsymbol{\lambda})$ in the joint space $\mathcal{X} \times \mathcal{L}$, that would require the computation of the covariance matrix $(c_t(\mathbf{x}_{j_1}, \mathbf{x}_{j_2}, \boldsymbol{\lambda}, \boldsymbol{\lambda}))_{j_1, j_2=1}^n$ when investigating the likelihood of $\boldsymbol{\lambda}$. Multi-output Gaussian processes [35–37] could be considered as well to account for the dependency between the outputs of the computer code $(f_t)_{t=1}^T$.

Even though the framework presented in this article is general, it has only been tested in the context of a transposition situation involving unobserved outputs. Other transposition cases should be explored, such as situations involving a change of scale where predictions are made at a point \mathbf{x}_0 far from the observation points $(\mathbf{x}_j)_{j=1}^n$. Note that the transposition situations can be combined as well, with a change of scale for \mathbf{x} and the prediction of an unobserved output y_t . The method with the hierarchical model and the different performance metrics remain valid in these contexts.

Finally, as previously mentioned, the results of the methods are highly influenced by the application test case. In particular, a computer code without constraints on the calibration variables would be valuable, as it would allow for the consideration of untruncated prior distributions for instance.

ACKNOWLEDGMENTS

This research was supported by the consortium in Applied Mathematics CIROQUO, gathering partners in technological and academia in the development of advanced methods for Computer Experiments (see <https://doi.org/10.5281/zenodo.6581217>).

References

1. Garrett, A., New, J., and Chandler, T., Evolutionary tuning of building models to monthly electrical consumption, *ASHRAE Transactions*, 119:89–100, 06 2013.
2. T. Agami Reddy, I.M. and Panjapornpon, C., Calibrating detailed building energy simulation programs with measured data—part ii: Application to three case study office buildings (rp-1051), *HVAC&R Research*, 13(2):243–265, 2007.
3. Muehleisen, R.T. and Bergerson, J., Bayesian calibration - what, why and how, In *Proceedings of the International High Performance Buildings Conference*, West Lafayette, Indiana, USA, 2016. Purdue University.
4. Kennedy, M.C. and O’Hagan, A., Bayesian calibration of computer models, *Journal of the Royal Statistical Society: Series B (Statistical Methodology)*, 63(3):425–464, 2001.
5. Higdon, D., Kennedy, M., Cavendish, J.C., Cafo, J.A., and Ryne, R.D., Combining field data and computer simulations for calibration and prediction, *SIAM Journal on Scientific Computing*, 26(2):448–466, 2004.
6. Bayarri, M., Berger, J., Paulo, R., Sacks, J., Kottas, A., and Tu, J., A framework for validation of computer models, *Technometrics*, 49:138–154, 05 2007.
7. Boukouvalas, A., Sykes, P., Cornford, D., and Maruri-Aguilar, H., Bayesian precalibration of a large stochastic microsimulation model, *IEEE Transactions on Intelligent Transportation Systems*, 15(3):1337–1347, 2014.
8. Campbell, K., Statistical calibration of computer simulations, *Reliability Engineering and System Safety*, 91(10):1358–1363, 2006, the Fourth International Conference on Sensitivity Analysis of Model Output (SAMO 2004).
9. O’Hagan, A., Bayesian inference with misspecified models: Inference about what?, *Journal of Statistical Planning and Inference*, 143(10):1643–1648, 2013.
10. Ling, Y., Mullins, J., and Mahadevan, S., Selection of model discrepancy priors in bayesian calibration, *Journal of Computational Physics*, 276:665–680, 2014.
11. Maupin, K.A. and Swiler, L.P., Model discrepancy calibration across experimental settings, *Reliability Engineering and System Safety*, 200:106818, 2020.
12. Oliver, T.A., Terejanu, G., Simmons, C.S., and Moser, R.D., Validating predictions of unobserved quantities, *Computer Methods in Applied Mechanics and Engineering*, 283:1310–1335, 2015.

13. Sargsyan, K., Huan, X., and Najm, H.N., Embedded model error representation for bayesian model calibration, *International Journal for Uncertainty Quantification*, 9(4):365–394, 2019.
14. Damblin, G. and Gaillard, P., Bayesian inference and non-linear extensions of the circe method for quantifying the uncertainty of closure relationships integrated into thermal-hydraulic system codes, *Nuclear Engineering and Design*, 359:110391, 2020.
15. van de Schoot, R., Depaoli, S., King, R., Kramer, B., Märtens, K., Tadesse, M.G., Vannucci, M., Gelman, A., Veen, D., Willemsen, J., , Bayesian statistics and modelling, *Nature Reviews Methods Primers*, 1(1):1, 2021.
16. Berkson, J., Bayes’ theorem, *The Annals of Mathematical Statistics*, 1(1):42–56, 1930.
17. Haario, H., Laine, M., Mira, A., and Saksman, E., Dram: efficient adaptive mcmc, *Statistics and computing*, 16:339–354, 2006.
18. Duane, S., Kennedy, A., Pendleton, B.J., and Roweth, D., Hybrid monte carlo, *Physics Letters B*, 195(2):216–222, 1987, [https://doi.org/10.1016/0370-2693\(87\)91197-X](https://doi.org/10.1016/0370-2693(87)91197-X).
19. Kemp, C., Perfors, A., and Tenenbaum, J.B., Learning overhypotheses with hierarchical bayesian models, *Developmental science*, 10(3):307–321, 2007.
20. Allenby, G.M. and Rossi, P.E., Hierarchical bayes models, *The handbook of marketing research: Uses, misuses, and future advances*, pp. 418–440, 2006.
21. Kloek, T. and van Dijk, H.K., Bayesian estimates of equation system parameters: An application of integration by monte carlo, *Econometrica*, 46(1):1–19, 1978.
22. Liu, D.C. and Nocedal, J., On the limited memory bfgs method for large scale optimization, *Mathematical programming*, 45(1):503–528, 1989.
23. Williams, C.K. and Rasmussen, C.E., *Gaussian processes for machine learning*, Vol. 2, MIT press Cambridge, MA, 2006.
24. Genton, M.G., Classes of kernels for machine learning: a statistics perspective, *J. Mach. Learn. Res.*, 2:299–312, mar 2002.
25. Weiss, N., Holmes, P., and Hardy, M., *A Course in Probability*, Pearson Addison Wesley, 2005.
26. Maudlin, P., Bingert, J., House, J., and Chen, S., On the modeling of the taylor cylinder impact test for orthotropic textured materials: experiments and simulations, *International Journal of Plasticity*, 15(2):139–166, 1999.
27. Burshtein, A.I., *Introduction to thermodynamics and kinetic theory of matter*, John Wiley & Sons, 2008.
28. Mai, J., Peng, L., Lin, Z., and Lai, X., Experimental study of electrical resistivity and flow stress of stainless steel 316l in electroplastic deformation, *Materials Science and Engineering: A*, 528(10-11):3539–3544, 2011.
29. McKay, M.D., Beckman, R.J., and Conover, W.J., A comparison of three methods for selecting values of input variables in the analysis of output from a computer code, *Technometrics*, 21(2):239–245, 1979.
30. Schaffer, T., Hensel, B., Weigand, C., Schüttler, J., and Jeleazcov, C., Evaluation of techniques for estimating the power spectral density of rr-intervals under paced respiration conditions, *Journal of clinical monitoring and computing*, 28:481–486, 2014.
31. Acharki, N., Bertinello, A., and Garnier, J., Robust prediction interval estimation for gaussian processes by cross-validation method, *Computational Statistics & Data Analysis*, 178:107597, 2023.
32. Miles, P.R., pymcstat: A python package for bayesian inference using delayed rejection adaptive metropolis, *Journal of Open Source Software*, 4(38):1417, 2019.
33. Richet, Y. and Have, P. libkriging, 2023. <https://github.com/libKriging/libKriging.git>.
34. SIRE, C. charliesire/supplementary_code_transposition, 2024. <https://doi.org/10.5281/zenodo.13685376>.
35. Le Gratiet, L. and Garnier, J., Recursive co-kriging model for design of computer experiments with multiple levels of fidelity, *International Journal for Uncertainty Quantification*, 4(5), 2014.
36. Alvarez, M.A., Rosasco, L., Lawrence, N.D., , Kernels for vector-valued functions: A review, *Foundations and Trends® in Machine Learning*, 4(3):195–266, 2012.
37. Gu, M. and Berger, J.O., Parallel partial Gaussian process emulation for computer models with massive output, *The Annals of Applied Statistics*, 10(3):1317 – 1347, 2016.

38. Korolev, V. and Shevtsova, I., An improvement of the berry–esseen inequality with applications to poisson and mixed poisson random sums, *Scandinavian Actuarial Journal*, 2012(2):81–105, 2012.
39. Vats, D., Flegal, J.M., and Jones, G.L., Strong consistency of multivariate spectral variance estimators in Markov chain Monte Carlo, *Bernoulli*, 24(3):1860 – 1909, 2018.
40. Terrell, G.R. and Scott, D.W., Variable kernel density estimation, *The Annals of Statistics*, pp. 1236–1265, 1992.
41. Wiener, N., The homogeneous chaos, *American Journal of Mathematics*, 60(4):897–936, 1938.

Appendix A. ESTIMATION OF THE CONFIDENCE LEVELS $\gamma(\alpha)$

We investigate a confidence level $\gamma(\alpha)$ associated with $p(\alpha | \mathbf{y}_{1,\text{obs}}) < \beta p(\alpha_\ell^* | \mathbf{y}_{1,\text{obs}})$ for a given α , which is equivalent to a confidence level for $p(\mathbf{y}_{1,\text{obs}} | \alpha)p_{\mathbf{A}}(\alpha) < \beta p(\mathbf{y}_{1,\text{obs}} | \alpha_\ell^*)p_{\mathbf{A}}(\alpha_\ell^*)$. We introduce:

$$\begin{cases} \mu(\alpha) = p(\mathbf{y}_{1,\text{obs}} | \alpha)p_{\mathbf{A}}(\alpha) - \beta p(\mathbf{y}_{1,\text{obs}} | \alpha_\ell^*)p_{\mathbf{A}}(\alpha_\ell^*) \\ v_\beta(\alpha) = \mathbb{V}_{\alpha_\ell^*} \left(p(\mathbf{y}_{1,\text{obs}} | \Lambda) \frac{p_{\Lambda}(\Lambda | \alpha)p_{\mathbf{A}}(\alpha) - \beta p_{\Lambda}(\Lambda | \alpha_\ell^*)p_{\mathbf{A}}(\alpha_\ell^*)}{p_{\Lambda}(\Lambda | \alpha_\ell^*)} \right), \end{cases}$$

where Λ has pdf $p_{\Lambda}(\cdot | \alpha_\ell^*)$, and

$$S_{L'}(\alpha)^2 = \frac{1}{L' - 1} \sum_{k=1}^{L'} \left(p(\mathbf{y}_{1,\text{obs}} | \Lambda'_k) \frac{p_{\Lambda}(\Lambda'_k | \alpha)p_{\mathbf{A}}(\alpha) - \beta p_{\Lambda}(\Lambda'_k | \alpha_\ell^*)p_{\mathbf{A}}(\alpha_\ell^*)}{p_{\Lambda}(\Lambda'_k | \alpha_\ell^*)} - \left(\hat{P}_{L'}^{\alpha_\ell^*}(\mathbf{y}_{1,\text{obs}} | \alpha)p_{\mathbf{A}}(\alpha) - \beta \hat{P}_{L'}^{\alpha_\ell^*}(\mathbf{y}_{1,\text{obs}} | \alpha_\ell^*)p_{\mathbf{A}}(\alpha_\ell^*) \right) \right)^2.$$

From the law of large numbers, $S_{L'}(\alpha)^2 \xrightarrow[L' \rightarrow \infty]{p} v_\beta(\alpha)$ and then $\frac{S_{L'}(\alpha)}{\sqrt{v_\beta(\alpha)}} \xrightarrow[L' \rightarrow \infty]{p} 1$. The Central Limit Theorem [38] provides that, given α_ℓ^* , for $(\Lambda'_k)_{k=1}^{L'}$ i.i.d. with pdf $p_{\Lambda}(\cdot | \alpha_\ell^*)$ and $\hat{P}_{L'}^{\alpha_\ell^*}(\mathbf{y}_{1,\text{obs}} | \alpha)$ defined by Equation (7),

$$\frac{\sqrt{L'} \left(\hat{P}_{L'}^{\alpha_\ell^*}(\mathbf{y}_{1,\text{obs}} | \alpha)p_{\mathbf{A}}(\alpha) - \beta \hat{P}_{L'}^{\alpha_\ell^*}(\mathbf{y}_{1,\text{obs}} | \alpha_\ell^*)p_{\mathbf{A}}(\alpha_\ell^*) - \mu(\alpha) \right)}{\sqrt{v_\beta(\alpha)}} \xrightarrow[L' \rightarrow \infty]{d} \mathcal{N}(0, 1).$$

Slutsky's theorem then provides

$$\frac{\sqrt{L'} \left(\hat{P}_{L'}^{\alpha_\ell^*}(\mathbf{y}_{1,\text{obs}} | \alpha)p_{\mathbf{A}}(\alpha) - \beta \hat{P}_{L'}^{\alpha_\ell^*}(\mathbf{y}_{1,\text{obs}} | \alpha_\ell^*)p_{\mathbf{A}}(\alpha_\ell^*) - \mu(\alpha) \right)}{S_{L'}(\alpha)} \xrightarrow[L' \rightarrow \infty]{d} \mathcal{N}(0, 1). \quad (\text{A.1})$$

We introduce the hypothesis of a statistical test $H_0 : \mu(\alpha) \geq 0$. We consider $\gamma(\alpha)$ the complementary of the associated p-value, defined by

$$\gamma(\alpha) = 1 - \mathbb{P} \left[\frac{\hat{P}_{L'}^{\alpha_\ell^*}(\mathbf{y}_{1,\text{obs}} | \alpha)p_{\mathbf{A}}(\alpha) - \beta \hat{P}_{L'}^{\alpha_\ell^*}(\mathbf{y}_{1,\text{obs}} | \alpha_\ell^*)p_{\mathbf{A}}(\alpha_\ell^*)}{S_{L'}(\alpha)} \leq \frac{\hat{P}_{L'}^{\alpha_\ell^*}(\mathbf{y}_{1,\text{obs}} | \alpha)p_{\mathbf{A}}(\alpha) - \beta \hat{P}_{L'}^{\alpha_\ell^*}(\mathbf{y}_{1,\text{obs}} | \alpha_\ell^*)p_{\mathbf{A}}(\alpha_\ell^*)}{S_{L'}(\alpha)} \right]$$

under $\mu(\alpha) = 0$, with $s_{L'}(\alpha)$, $\hat{p}_{L'}^{\alpha_\ell^*}(\mathbf{y}_{1,\text{obs}} \mid \alpha_\ell^*)$ and $\hat{p}_{L'}^{\alpha_\ell^*}(\mathbf{y}_{1,\text{obs}} \mid \alpha)$ the obtained realizations of the associated estimators. Then, $\gamma(\alpha)$ is indeed a confidence level associated with $\mu(\alpha) < 0$, the alternative hypothesis. Under $\mu(\alpha) = 0$, with Equation A.1, we have for $z \in \mathbb{R}$,

$$\mathbb{P} \left[\frac{\hat{P}_{L'}^{\alpha_\ell^*}(\mathbf{y}_{1,\text{obs}} \mid \alpha) p_{\mathbf{A}}(\alpha) - \beta \hat{P}_{L'}^{\alpha_\ell^*}(\mathbf{y}_{1,\text{obs}} \mid \alpha_\ell^*) p_{\mathbf{A}}(\alpha_\ell^*)}{s_{L'}(\alpha)} \leq \frac{z}{\sqrt{L'}} \right] \xrightarrow{L' \rightarrow \infty} \Phi(z).$$

with Φ is the cdf of a Gaussian distribution with mean 0 and variance 1.

Finally, with $z = \frac{\sqrt{L'} \left(\hat{p}_{L'}^{\alpha_\ell^*}(\mathbf{y}_{1,\text{obs}} \mid \alpha) p_{\mathbf{A}}(\alpha) - \beta \hat{p}_{L'}^{\alpha_\ell^*}(\mathbf{y}_{1,\text{obs}} \mid \alpha_\ell^*) p_{\mathbf{A}}(\alpha_\ell^*) \right)}{s_{L'}(\alpha)}$, we have the following asymptotic approximation for the confidence level

$$\gamma(\alpha) = \Phi \left(\frac{\sqrt{L'} \left(\beta \hat{p}_{L'}^{\alpha_\ell^*}(\mathbf{y}_{1,\text{obs}} \mid \alpha_\ell^*) p_{\mathbf{A}}(\alpha_\ell^*) - \hat{p}_{L'}^{\alpha_\ell^*}(\mathbf{y}_{1,\text{obs}} \mid \alpha) p_{\mathbf{A}}(\alpha) \right)}{s_{L'}(\alpha)} \right). \quad (\text{A.2})$$

Appendix B. THEOREMS FOR ALMOST SURE INTERCHANGE OF LIMIT AND INTEGRAL

Theorem 1. Let $(u_L)_{L \in \mathbb{N}}$ a sequence of functions with $u_L : \mathcal{A} \rightarrow \mathbb{R}$. If

1. \mathcal{A} is convex
2. $\forall L$, u_L is continuous on \mathcal{A} , and the first derivatives of u_L are defined
3. $\exists C > 0$, $\exists L_0 \in \mathbb{N}$, $\forall L > L_0$, $\forall \alpha \in \mathcal{A}$, $\|\nabla u_L(\alpha)\| < C$

Then, $(u_L)_{L > L_0}$ is uniformly equicontinuous.

Proof. Let $\epsilon > 0$. For $(\alpha_1, \alpha_2) \in \mathcal{A}^2$, we denote by $G(\alpha_1, \alpha_2)$ the line segment with α_1 and α_2 as endpoints. The mean value theorem for multivariate functions gives

$$\forall L > L_0, \forall (\alpha_1, \alpha_2) \in \mathcal{A}^2, \exists \mathbf{c} \in G(\alpha_1, \alpha_2), \|u_L(\alpha_2) - u_L(\alpha_1)\| = \|\nabla u_L(\mathbf{c}) \cdot (\alpha_2 - \alpha_1)\| \leq C \|\alpha_2 - \alpha_1\|$$

Then,

$$\|\alpha_2 - \alpha_1\| < \frac{\epsilon}{C} \Rightarrow \forall L > L_0, \|u_L(\alpha_2) - u_L(\alpha_1)\| < \epsilon.$$

□

Corollary 1. Under the same hypothesis as Theorem 1, if we additionally suppose that

1. \mathbb{Q} is dense in \mathcal{A}
2. $\forall \alpha \in \mathbb{Q} \cap \mathcal{A}$, $u_L(\alpha) \xrightarrow{L \rightarrow \infty} u(\alpha)$
3. u is continuous on \mathcal{A}

Then, $\forall \alpha \in \mathcal{A}$, $u_L(\alpha) \xrightarrow{L \rightarrow \infty} u(\alpha)$

Proof. Let $\alpha \in \mathcal{A}$ and $\epsilon > 0$. From Theorem 1,

$$\|\tilde{\alpha} - \alpha\| < \frac{\epsilon}{3C} \Rightarrow \forall L > L_0, \|u_L(\tilde{\alpha}) - u_L(\alpha)\| < \frac{\epsilon}{3}. \quad (\text{B.1})$$

From the continuity of u ,

$$\exists \eta > 0, \|\tilde{\alpha} - \alpha\| < \eta \Rightarrow \|u(\tilde{\alpha}) - u(\alpha)\| < \frac{\epsilon}{3}. \quad (\text{B.2})$$

From the convergence in \mathbb{Q} ,

$$\tilde{\alpha} \in \mathbb{Q} \Rightarrow \exists L_{\tilde{\alpha}} \in \mathbb{N}, \forall L > L_{\tilde{\alpha}}, \|u_L(\tilde{\alpha}) - u(\tilde{\alpha})\| < \frac{\epsilon}{3}. \quad (\text{B.3})$$

As \mathbb{Q} is dense in \mathcal{A} , then $\exists \tilde{\alpha} \in \mathbb{Q}, \|\tilde{\alpha} - \alpha\| < \min(\eta, \frac{\epsilon}{3C})$. From Equations B.1, B.2, B.3, $\exists L_{\tilde{\alpha}} \in \mathbb{N}, \forall L > \max(L_{\tilde{\alpha}}, L_0)$,

$$\|u_L(\alpha) - u(\alpha)\| \leq \|u_L(\alpha) - u_L(\tilde{\alpha})\| + \|u_L(\tilde{\alpha}) - u(\tilde{\alpha})\| + \|u(\tilde{\alpha}) - u(\alpha)\| < \epsilon \quad (\text{B.4})$$

□

Theorem 2. Let $(U_L)_{L \in \mathbb{N}}$ a sequence such that $\forall L \in \mathbb{N}, \{U_L(\alpha), \alpha \in \mathcal{A}\}$ is a stochastic process, and z a function of α . If

1. \mathcal{A} is convex and \mathbb{Q} is dense in \mathcal{A}
2. $\forall \alpha \in \mathcal{A}, \mathbb{P}(U_L(\alpha) \xrightarrow{L \rightarrow \infty} u(\alpha)) = 1$
3. $\mathbb{P}(\forall L \in \mathbb{N}, U_L \text{ is continuous and its first derivatives are defined}) = 1$
4. $\exists C > 0, \mathbb{P}(\exists L_0 \in \mathbb{N}, \forall L > L_0, \forall \alpha \in \mathcal{A}, \|\nabla U_L(\alpha)\| < C) = 1$
5. $\exists v$ integrable, $\mathbb{P}(\exists L_1 \in \mathbb{N}, \forall L > L_1, \forall \alpha, |U_L(\alpha)z(\alpha)| \leq v(\alpha)) = 1$
6. u is continuous

Then, $\int_{\mathcal{A}} U_L(\alpha)z(\alpha)d\alpha \xrightarrow{L \rightarrow \infty, a.s.} \int_{\mathcal{A}} u(\alpha)z(\alpha)d\alpha$.

Proof. We have

- $\mathbb{P}\left(\bigcap_{\alpha \in \mathbb{Q} \cap \mathcal{A}} \left\{U_L(\alpha) \xrightarrow{L \rightarrow \infty} u(\alpha)\right\}\right) = 1$ from hypothesis 2.
- $\mathbb{P}\left(\bigcap_{L \in \mathbb{N}} \{U_L \text{ is continuous and its first derivatives are defined}\}\right) = 1$ from hypothesis 3.
- $\exists C > 0, \mathbb{P}\left(\exists L_0 \in \mathbb{N}, \bigcap_{L > L_0} \{\forall \alpha \in \mathcal{A}, \|\nabla U_L(\alpha)\| < C\}\right) = 1$ from hypothesis 4.

Then, from Corollary 1, $\mathbb{P}\left(\left\{\forall \alpha \in \mathcal{A}, U_L(\alpha)z(\alpha) \xrightarrow{L \rightarrow \infty} u(\alpha)z(\alpha)\right\}\right) = 1$

Hypothesis 5 leads to

$$\mathbb{P}\left(\exists L_1 \in \mathbb{N}, \bigcap_{L > L_1} \{\forall \alpha, |U_L(\alpha)z(\alpha)| \leq v(\alpha)\}\right) = 1$$

Then the dominated convergence theorem gives

$$\mathbb{P}\left(\int_{\mathcal{A}} U_L(\alpha)z(\alpha)d\alpha \xrightarrow{L \rightarrow \infty} \int_{\mathcal{A}} u(\alpha)z(\alpha)d\alpha\right) = 1.$$

□

Appendix C. CONSISTENCY OF $\int_{\mathcal{A}} \mathbb{E}(h(\Lambda) \mid \alpha, \mathbf{y}_{1,\text{obs}}) \hat{P}_L^{\alpha_\ell^*}(\alpha \mid \mathbf{y}_{1,\text{obs}}) d\alpha$

We have $\hat{P}_L^{\alpha_\ell^*}(\alpha \mid \mathbf{y}_{1,\text{obs}}) = \frac{\hat{P}_L^{\alpha_\ell^*}(\mathbf{y}_{1,\text{obs}} \mid \alpha) p_{\mathbf{A}}(\alpha)}{\int_{\mathcal{A}} \hat{P}_L^{\alpha_\ell^*}(\mathbf{y}_{1,\text{obs}} \mid \alpha') p_{\mathbf{A}}(\alpha') d\alpha'}$ where $\hat{P}_L^{\alpha_\ell^*}(\mathbf{y}_{1,\text{obs}} \mid \alpha)$ is defined by Equation (7) for all α with $\alpha^* = \alpha_\ell^*$ and $(\Lambda'_k)_{k=1}^L$ i.i.d. with pdf $p_{\Lambda}(\cdot \mid \alpha_\ell^*)$.

We assume that

1. \mathcal{A} is convex and \mathbb{Q} is dense in \mathcal{A}
2. $\exists \mathcal{K}$ compact set, $\forall \alpha \in \mathcal{A}$, $\text{supp}(p_{\Lambda}(\cdot \mid \alpha)) = \mathcal{K}$.
3. h is continuous on \mathcal{K} , and then bounded by a constant b_0 .
4. $\lambda \mapsto p(\mathbf{y}_{1,\text{obs}} \mid \lambda)$ is continuous on \mathcal{K} , and then bounded by a constant b_1 .
5. $\forall \alpha \in \mathcal{A}$, $p_{\Lambda}(\cdot \mid \alpha)$ is continuous almost everywhere on \mathcal{K} .
6. $\exists b_2 > 0$, $\forall \alpha \in \mathcal{A}$, $p_{\Lambda}(\cdot \mid \alpha)$ is bounded by b_2 on \mathcal{K} .
7. $\exists b_3 > 0$, $\forall \alpha \in \mathcal{A}, \forall \lambda \in \mathcal{K}$, $p_{\Lambda}(\lambda \mid \alpha) > b_3$.
8. $\forall \lambda \in \mathcal{K}$, $p_{\Lambda}(\lambda \mid \cdot)$ is continuous, its first derivatives are defined and $\exists b_4 > 0, \forall \lambda \in \mathcal{K}, \forall \alpha \in \mathcal{A}$, $\|\nabla_{\alpha} p(\lambda \mid \alpha)\| < b_4$.

This proof is structured as follows:

- Show that $\int_{\mathcal{A}} \hat{P}_L^{\alpha_\ell^*}(\mathbf{y}_{1,\text{obs}} \mid \alpha') p_{\mathbf{A}}(\alpha') d\alpha' \xrightarrow[L \rightarrow \infty]{a.s.} \int_{\mathcal{A}} p(\mathbf{y}_{1,\text{obs}} \mid \alpha') p_{\mathbf{A}}(\alpha') d\alpha'$
- Show that $\hat{P}_L^{\alpha_\ell^*}(\alpha \mid \mathbf{y}_{1,\text{obs}}) \xrightarrow[L \rightarrow \infty]{a.s.} p(\alpha \mid \mathbf{y}_{1,\text{obs}})$
- Show that $\int_{\mathcal{A}} \mathbb{E}(h(\Lambda) \mid \alpha, \mathbf{y}_{1,\text{obs}}) \hat{P}_L^{\alpha_\ell^*}(\alpha \mid \mathbf{y}_{1,\text{obs}}) d\alpha \xrightarrow[L \rightarrow \infty]{a.s.} \int_{\mathcal{A}} \mathbb{E}(h(\Lambda) \mid \alpha, \mathbf{y}_{1,\text{obs}}) p(\alpha \mid \mathbf{y}_{1,\text{obs}}) d\alpha$

Appendix C.1 Convergence of $\int_{\mathcal{A}} \hat{P}_L^{\alpha_\ell^*}(\mathbf{y}_{1,\text{obs}} \mid \alpha') p_{\mathbf{A}}(\alpha') d\alpha'$

We have:

- $\forall \alpha \in \mathcal{A}$, $\mathbb{P}\left(\hat{P}_L^{\alpha_\ell^*}(\mathbf{y}_{1,\text{obs}} \mid \alpha) \xrightarrow[L \rightarrow \infty]{} p(\mathbf{y}_{1,\text{obs}} \mid \alpha)\right) = 1$ from the strong law of large numbers.
- $\mathbb{P}\left(\forall L \in \mathbb{N}, \bigcap_{k=1}^L \{\Lambda'_k \in \mathcal{K}\}\right) = 1$ and then
 - $\mathbb{P}\left(\forall L \in \mathbb{N}, \alpha \mapsto \hat{P}_L^{\alpha_\ell^*}(\mathbf{y}_{1,\text{obs}} \mid \alpha) \text{ is continuous on } \mathcal{A}\right) = 1$ from the continuity of $p_{\Lambda}(\lambda \mid \cdot)$ for $\lambda \in \mathcal{K}$.
 - $\mathbb{P}\left(\forall L \in \mathbb{N}, \forall \alpha \in \mathcal{A}, \forall 1 \leq a \leq r, \left| \frac{\partial \hat{P}_L^{\alpha_\ell^*}(\mathbf{y}_{1,\text{obs}} \mid \alpha)}{\partial \alpha_a} \right| \leq \frac{b_1 b_4}{b_3}\right) = 1$.
 - $\mathbb{P}\left(\forall L \in \mathbb{N}, \forall \alpha \in \mathcal{A}, \left| \hat{P}_L^{\alpha_\ell^*}(\mathbf{y}_{1,\text{obs}} \mid \alpha) p_{\mathbf{A}}(\alpha) \right| \leq \frac{b_1 b_2}{b_3} p_{\mathbf{A}}(\alpha)\right) = 1$.
- $\alpha \mapsto p(\mathbf{y}_{1,\text{obs}} \mid \alpha) = \int_{\mathcal{K}} p(\mathbf{y}_{1,\text{obs}} \mid \lambda) p(\lambda \mid \alpha) d\lambda$ is continuous on \mathcal{A} , as
 - $\forall \alpha \in \mathcal{A}, \lambda \mapsto p(\mathbf{y}_{1,\text{obs}} \mid \lambda) p(\lambda \mid \alpha)$ is continuous almost everywhere on \mathcal{K} .
 - $\forall \lambda \in \mathcal{K}, \alpha \mapsto p(\mathbf{y}_{1,\text{obs}} \mid \lambda) p(\lambda \mid \alpha)$ is continuous on \mathcal{A} .
 - $\forall \lambda \in \mathcal{K}, \forall \alpha \in \mathcal{A}, |p(\mathbf{y}_{1,\text{obs}} \mid \lambda) p(\lambda \mid \alpha)| \leq b_1 b_2$, with $b_1 b_2$ integrable on \mathcal{K} .

Then, from Theorem 2,

$$\int_{\mathcal{A}} \hat{P}_L^{\alpha_\ell^*}(\mathbf{y}_{1,\text{obs}} \mid \alpha) p_{\mathbf{A}}(\alpha) d\alpha \xrightarrow[L \rightarrow \infty]{a.s.} \int_{\mathcal{A}} p(\mathbf{y}_{1,\text{obs}} \mid \alpha) p_{\mathbf{A}}(\alpha) d\alpha. \quad (\text{C.1})$$

Appendix C.2 Convergence of $\hat{P}_L^{\alpha_\ell^*}(\boldsymbol{\alpha} \mid \mathbf{y}_{1,\text{obs}})$

The strong law of large numbers and Equation (C.1) provides, for $\boldsymbol{\alpha} \in \mathcal{A}$,

$$\begin{cases} \hat{P}_L^{\alpha_\ell^*}(\mathbf{y}_{1,\text{obs}} \mid \boldsymbol{\alpha}) p_{\mathbf{A}}(\boldsymbol{\alpha}) \xrightarrow[L \rightarrow \infty]{a.s.} p(\mathbf{y}_{1,\text{obs}} \mid \boldsymbol{\alpha}) p_{\mathbf{A}}(\boldsymbol{\alpha}), \\ \int_{\mathcal{A}} \hat{P}_L^{\alpha_\ell^*}(\mathbf{y}_{1,\text{obs}} \mid \boldsymbol{\alpha}') p_{\mathbf{A}}(\boldsymbol{\alpha}') d\boldsymbol{\alpha}' \xrightarrow[L \rightarrow \infty]{a.s.} \int_{\mathcal{A}} p(\mathbf{y}_{1,\text{obs}} \mid \boldsymbol{\alpha}') p_{\mathbf{A}}(\boldsymbol{\alpha}') d\boldsymbol{\alpha}'. \end{cases}$$

Then it comes

$$\hat{P}_L^{\alpha_\ell^*}(\boldsymbol{\alpha} \mid \mathbf{y}_{1,\text{obs}}) = \frac{\hat{P}_L^{\alpha_\ell^*}(\mathbf{y}_{1,\text{obs}} \mid \boldsymbol{\alpha}) p_{\mathbf{A}}(\boldsymbol{\alpha})}{\int_{\mathcal{A}} \hat{P}_L^{\alpha_\ell^*}(\mathbf{y}_{1,\text{obs}} \mid \boldsymbol{\alpha}') p_{\mathbf{A}}(\boldsymbol{\alpha}') d\boldsymbol{\alpha}'} \xrightarrow[L \rightarrow \infty]{a.s.} p(\boldsymbol{\alpha} \mid \mathbf{y}_{1,\text{obs}}). \quad (\text{C.2})$$

Appendix C.3 Convergence of $\int_{\mathcal{A}} \mathbb{E}(h(\boldsymbol{\Lambda}) \mid \boldsymbol{\alpha}, \mathbf{y}_{1,\text{obs}}) \hat{P}_L^{\alpha_\ell^*}(\boldsymbol{\alpha} \mid \mathbf{y}_{1,\text{obs}}) d\boldsymbol{\alpha}$

As from Equation (C.1),

$$\int_{\mathcal{A}} \hat{P}_L^{\alpha_\ell^*}(\mathbf{y}_{1,\text{obs}} \mid \boldsymbol{\alpha}') p_{\mathbf{A}}(\boldsymbol{\alpha}') d\boldsymbol{\alpha}' \xrightarrow[L \rightarrow \infty]{a.s.} \int_{\mathcal{A}} p(\mathbf{y}_{1,\text{obs}} \mid \boldsymbol{\alpha}') p_{\mathbf{A}}(\boldsymbol{\alpha}') d\boldsymbol{\alpha}'$$

then $\mathbb{P}\left(\exists L_0 \in \mathbb{N}, \forall L \geq L_0, \int_{\mathcal{A}} \hat{P}_L^{\alpha_\ell^*}(\mathbf{y}_{1,\text{obs}} \mid \boldsymbol{\alpha}') p_{\mathbf{A}}(\boldsymbol{\alpha}') d\boldsymbol{\alpha}' \geq \frac{1}{2} \int_{\mathcal{A}} p(\mathbf{y}_{1,\text{obs}} \mid \boldsymbol{\alpha}') p_{\mathbf{A}}(\boldsymbol{\alpha}') d\boldsymbol{\alpha}'\right) = 1$.

In this section, we denote $U_L(\boldsymbol{\alpha}) = \frac{\hat{P}_L^{\alpha_\ell^*}(\mathbf{y}_{1,\text{obs}} \mid \boldsymbol{\alpha})}{\int_{\mathcal{A}} \hat{P}_L^{\alpha_\ell^*}(\mathbf{y}_{1,\text{obs}} \mid \boldsymbol{\alpha}') p_{\mathbf{A}}(\boldsymbol{\alpha}') d\boldsymbol{\alpha}'}$.

We have:

- $\forall \boldsymbol{\alpha} \in \mathcal{A}, U_L(\boldsymbol{\alpha}) \xrightarrow[L \rightarrow \infty]{a.s.} \frac{p(\mathbf{y}_{1,\text{obs}} \mid \boldsymbol{\alpha})}{\int_{\mathcal{A}} p(\mathbf{y}_{1,\text{obs}} \mid \boldsymbol{\alpha}') p_{\mathbf{A}}(\boldsymbol{\alpha}') d\boldsymbol{\alpha}'}$
- $\mathbb{P}\left(\forall L \in \mathbb{N}, \bigcap_{k=1}^L \{\boldsymbol{\Lambda}'_k \in \mathcal{K}\}\right) = 1$ and then
 - $\mathbb{P}(\forall L \in \mathbb{N}, U_L \text{ is continuous on } \mathcal{A}) = 1$ from the continuity of $p(\boldsymbol{\lambda} \mid \cdot)$ for $\boldsymbol{\lambda} \in \mathcal{K}$.
 - $\mathbb{P}\left(\exists L_0 \in \mathbb{N}, \forall L > L_0, \forall \boldsymbol{\alpha} \in \mathcal{A}, \forall 1 \leq a \leq r, \left| \frac{\partial U_L(\boldsymbol{\alpha})}{\partial \alpha_a} \right| \leq 2 \frac{\frac{b_1 b_4}{b_3}}{\int_{\mathcal{A}} p(\mathbf{y}_{1,\text{obs}} \mid \boldsymbol{\alpha}') p_{\mathbf{A}}(\boldsymbol{\alpha}') d\boldsymbol{\alpha}'}\right) = 1$.
 - $\mathbb{P}\left(\exists L_0 \in \mathbb{N}, \forall L > L_0, \forall \boldsymbol{\alpha} \in \mathcal{A}, |\mathbb{E}(h(\boldsymbol{\Lambda}) \mid \boldsymbol{\alpha}, \mathbf{y}_{1,\text{obs}}) p_{\mathbf{A}}(\boldsymbol{\alpha}) U_L(\boldsymbol{\alpha})| \leq 2b_0 p_{\mathbf{A}}(\boldsymbol{\alpha}) \frac{\frac{b_1 b_2}{b_3}}{\int_{\mathcal{A}} p(\mathbf{y}_{1,\text{obs}} \mid \boldsymbol{\alpha}') p_{\mathbf{A}}(\boldsymbol{\alpha}') d\boldsymbol{\alpha}'}\right) = 1$.
- $\boldsymbol{\alpha} \mapsto \frac{p(\mathbf{y}_{1,\text{obs}} \mid \boldsymbol{\alpha})}{\int_{\mathcal{A}} \hat{P}_L^{\alpha_\ell^*}(\mathbf{y}_{1,\text{obs}} \mid \boldsymbol{\alpha}') p_{\mathbf{A}}(\boldsymbol{\alpha}') d\boldsymbol{\alpha}'}$ is continuous

Then, from Theorem 2, as $\mathbb{E}(h(\boldsymbol{\Lambda}) \mid \boldsymbol{\alpha}, \mathbf{y}_{1,\text{obs}}) \hat{P}_L^{\alpha_\ell^*}(\boldsymbol{\alpha} \mid \mathbf{y}_{1,\text{obs}}) = \mathbb{E}(h(\boldsymbol{\Lambda}) \mid \boldsymbol{\alpha}, \mathbf{y}_{1,\text{obs}}) p_{\mathbf{A}}(\boldsymbol{\alpha}) U_L(\boldsymbol{\alpha})$,

$$\int_{\mathcal{A}} \mathbb{E}(h(\boldsymbol{\Lambda}) \mid \boldsymbol{\alpha}, \mathbf{y}_{1,\text{obs}}) \hat{P}_L^{\alpha_\ell^*}(\boldsymbol{\alpha} \mid \mathbf{y}_{1,\text{obs}}) d\boldsymbol{\alpha} \xrightarrow[L \rightarrow \infty]{a.s.} \int_{\mathcal{A}} \mathbb{E}(h(\boldsymbol{\Lambda}) \mid \boldsymbol{\alpha}, \mathbf{y}_{1,\text{obs}}) p(\boldsymbol{\alpha} \mid \mathbf{y}_{1,\text{obs}}) d\boldsymbol{\alpha}. \quad (\text{C.3})$$

Appendix D. CONSISTENCY OF $\hat{E}_{N,M}^{\alpha_\ell^*}(h(\boldsymbol{\Lambda}))$

We investigate the convergence of

$$\hat{E}_{N,M}^{\alpha_\ell^*}(h(\boldsymbol{\Lambda})) = \frac{1}{N} \sum_{i=1}^N \frac{\sum_{k=1}^M h(\boldsymbol{\Lambda}_k) \frac{p_{\mathbf{A}}(\boldsymbol{\Lambda}_k \mid \mathbf{A}_i)}{p_{\mathbf{A}}(\boldsymbol{\Lambda}_k \mid \boldsymbol{\alpha}_\ell^*)}}{\sum_{k=1}^M \frac{p_{\mathbf{A}}(\boldsymbol{\Lambda}_k \mid \mathbf{A}_i)}{p_{\mathbf{A}}(\boldsymbol{\Lambda}_k \mid \boldsymbol{\alpha}_\ell^*)}} \quad (\text{D.1})$$

for every h function of $\mathbf{\Lambda}$ continuous, bounded on \mathcal{K} , with $(\mathbf{A}_i)_{i=1}^N$ sampled with pdf proportional to $\hat{p}_L^{\alpha_\ell^*}(\mathbf{y}_{1,\text{obs}} \mid \boldsymbol{\alpha})p_{\mathbf{A}}(\boldsymbol{\alpha})$ and $(\mathbf{\Lambda}_k)_{k=1}^M$ sampled with pdf proportional to $p(\mathbf{y}_{1,\text{obs}} \mid \boldsymbol{\lambda})p_{\mathbf{\Lambda}}(\boldsymbol{\lambda} \mid \boldsymbol{\alpha}_\ell^*)$. Note that here, $\hat{p}_L^{\alpha_\ell^*}(\mathbf{y}_{1,\text{obs}} \mid \boldsymbol{\alpha})$ is considered known and thus is deterministic, the convergence is related to the samples $(\mathbf{A}_i)_{i=1}^N$ and $(\mathbf{\Lambda}_k)_{k=1}^M$. We suppose that the hypothesis of Appendix C are verified.

Let us denote

$$\hat{E}_M^{\alpha_\ell^*}(h(\mathbf{\Lambda}), \boldsymbol{\alpha}) = \frac{\sum_{k=1}^M h(\mathbf{\Lambda}_k) \frac{p_{\mathbf{\Lambda}}(\mathbf{\Lambda}_k \mid \boldsymbol{\alpha})}{p_{\mathbf{\Lambda}}(\mathbf{\Lambda}_k \mid \boldsymbol{\alpha}_\ell^*)}}{\sum_{k=1}^M \frac{p_{\mathbf{\Lambda}}(\mathbf{\Lambda}_k \mid \boldsymbol{\alpha})}{p_{\mathbf{\Lambda}}(\mathbf{\Lambda}_k \mid \boldsymbol{\alpha}_\ell^*)}}.$$

Then,

$$\hat{E}_{N,M}^{\alpha_\ell^*}(h(\mathbf{\Lambda})) = \frac{1}{N} \sum_{i=1}^N \hat{E}_M^{\alpha_\ell^*}(h(\mathbf{\Lambda}), \mathbf{A}_i).$$

Let us show that $\hat{E}_{N,M}^{\alpha_\ell^*}(h(\mathbf{\Lambda}))$ is a consistent estimator of $\int_{\mathcal{A}} \mathbb{E}(h(\mathbf{\Lambda}) \mid \boldsymbol{\alpha}, \mathbf{y}_{1,\text{obs}}) \hat{p}_L^{\alpha_\ell^*}(\boldsymbol{\alpha} \mid \mathbf{y}_{1,\text{obs}}) d\boldsymbol{\alpha}$, with

$$\mathbb{E}(h(\mathbf{\Lambda}) \mid \boldsymbol{\alpha}, \mathbf{y}_{1,\text{obs}}) = \frac{\int_{\mathbb{R}^q} h(\boldsymbol{\lambda}) p(\mathbf{y}_{1,\text{obs}} \mid \boldsymbol{\lambda}) \frac{p_{\mathbf{\Lambda}}(\boldsymbol{\lambda} \mid \boldsymbol{\alpha})}{p_{\mathbf{\Lambda}}(\boldsymbol{\lambda} \mid \boldsymbol{\alpha}_\ell^*)} p_{\mathbf{\Lambda}}(\boldsymbol{\lambda} \mid \boldsymbol{\alpha}_\ell^*) d\boldsymbol{\lambda}}{\int_{\mathbb{R}^q} p(\mathbf{y}_{1,\text{obs}} \mid \boldsymbol{\lambda}) \frac{p_{\mathbf{\Lambda}}(\boldsymbol{\lambda} \mid \boldsymbol{\alpha})}{p_{\mathbf{\Lambda}}(\boldsymbol{\lambda} \mid \boldsymbol{\alpha}_\ell^*)} p_{\mathbf{\Lambda}}(\boldsymbol{\lambda} \mid \boldsymbol{\alpha}_\ell^*) d\boldsymbol{\lambda}}.$$

More precisely, we will investigate

- $\lim_{M \rightarrow \infty} \lim_{N \rightarrow \infty} \hat{E}_{N,M}^{\alpha_\ell^*}(h(\mathbf{\Lambda}))$
- $\lim_{N \rightarrow \infty} \lim_{M \rightarrow \infty} \hat{E}_{N,M}^{\alpha_\ell^*}(h(\mathbf{\Lambda}))$

Appendix D.1 Almost sure $\lim_{M \rightarrow \infty} \lim_{N \rightarrow \infty} \hat{E}_{N,M}^{\alpha_\ell^*}(h(\mathbf{\Lambda}))$

This proof is structured as follows:

- Show that $\hat{E}_M^{\alpha_\ell^*}(h(\mathbf{\Lambda}), \boldsymbol{\alpha}) \xrightarrow[M \rightarrow \infty]{a.s.} \mathbb{E}(h(\mathbf{\Lambda}) \mid \boldsymbol{\alpha}, \mathbf{y}_{1,\text{obs}})$
- Show that it brings $\int_{\mathcal{A}} \hat{E}_M^{\alpha_\ell^*}(h(\mathbf{\Lambda}), \boldsymbol{\alpha}) \hat{p}_L^{\alpha_\ell^*}(\boldsymbol{\alpha} \mid \mathbf{y}_{1,\text{obs}}) d\boldsymbol{\alpha} \xrightarrow[M \rightarrow \infty]{a.s.} \int_{\mathcal{A}} \mathbb{E}(h(\mathbf{\Lambda}) \mid \boldsymbol{\alpha}, \mathbf{y}_{1,\text{obs}}) \hat{p}_L^{\alpha_\ell^*}(\boldsymbol{\alpha} \mid \mathbf{y}_{1,\text{obs}}) d\boldsymbol{\alpha}$
- Show that $\hat{E}_{N,M}^{\alpha_\ell^*}(h(\mathbf{\Lambda})) \xrightarrow[N \rightarrow \infty]{a.s.} \int_{\mathcal{A}} \hat{E}_M^{\alpha_\ell^*}(h(\mathbf{\Lambda}), \boldsymbol{\alpha}) \hat{p}_L^{\alpha_\ell^*}(\boldsymbol{\alpha} \mid \mathbf{y}_{1,\text{obs}}) d\boldsymbol{\alpha}$
- Conclude that $\mathbb{P}\left(\lim_{M \rightarrow \infty} \lim_{N \rightarrow \infty} \hat{E}_{N,M}^{\alpha_\ell^*}(h(\mathbf{\Lambda})) = \int_{\mathcal{A}} \mathbb{E}(h(\mathbf{\Lambda}) \mid \boldsymbol{\alpha}, \mathbf{y}_{1,\text{obs}}) \hat{p}_L^{\alpha_\ell^*}(\boldsymbol{\alpha} \mid \mathbf{y}_{1,\text{obs}}) d\boldsymbol{\alpha}\right) = 1$

Appendix D.1.1 Almost sure convergence of $\hat{E}_M^{\alpha_\ell^*}(h(\mathbf{\Lambda}), \boldsymbol{\alpha})$ to $\mathbb{E}(h(\mathbf{\Lambda}) \mid \boldsymbol{\alpha}, \mathbf{y}_{1,\text{obs}})$.

Let $\boldsymbol{\alpha} \in \mathcal{A}$.

$$\mathbb{E}(h(\mathbf{\Lambda}) \mid \boldsymbol{\alpha}, \mathbf{y}_{1,\text{obs}}) = \frac{\int_{\mathbb{R}^q} h(\boldsymbol{\lambda}) \frac{p_{\mathbf{\Lambda}}(\boldsymbol{\lambda} \mid \boldsymbol{\alpha})}{p_{\mathbf{\Lambda}}(\boldsymbol{\lambda} \mid \boldsymbol{\alpha}_{\ell}^*)} p(\mathbf{y}_{1,\text{obs}} \mid \boldsymbol{\lambda}) p_{\mathbf{\Lambda}}(\boldsymbol{\lambda} \mid \boldsymbol{\alpha}_{\ell}^*) d\boldsymbol{\lambda}}{\underbrace{\int_{\mathbb{R}^q} p(\mathbf{y}_{1,\text{obs}} \mid \boldsymbol{\lambda}) p_{\mathbf{\Lambda}}(\boldsymbol{\lambda} \mid \boldsymbol{\alpha}_{\ell}^*) d\boldsymbol{\lambda}}_{=I_1}} \times \frac{\int_{\mathbb{R}^q} p(\mathbf{y}_{1,\text{obs}} \mid \boldsymbol{\lambda}) p_{\mathbf{\Lambda}}(\boldsymbol{\lambda} \mid \boldsymbol{\alpha}_{\ell}^*) d\boldsymbol{\lambda}}{\underbrace{\int_{\mathbb{R}^q} \frac{p_{\mathbf{\Lambda}}(\boldsymbol{\lambda} \mid \boldsymbol{\alpha})}{p_{\mathbf{\Lambda}}(\boldsymbol{\lambda} \mid \boldsymbol{\alpha}_{\ell}^*)} p(\mathbf{y}_{1,\text{obs}} \mid \boldsymbol{\lambda}) p_{\mathbf{\Lambda}}(\boldsymbol{\lambda} \mid \boldsymbol{\alpha}_{\ell}^*) d\boldsymbol{\lambda}}_{=I_2}}.$$

As explained in [39], MCMC simulates $(\mathbf{\Lambda}_k)_{k=1}^M$ which is a Harris ergodic Markov Chain with invariant distribution $\frac{p(\mathbf{y}_{1,\text{obs}} \mid \boldsymbol{\lambda}) p_{\mathbf{\Lambda}}(\boldsymbol{\lambda} \mid \boldsymbol{\alpha}_{\ell}^*)}{\int_{\mathbb{R}^q} p(\mathbf{y}_{1,\text{obs}} \mid \boldsymbol{\lambda}') p_{\mathbf{\Lambda}}(\boldsymbol{\lambda}' \mid \boldsymbol{\alpha}_{\ell}^*) d\boldsymbol{\lambda}'}$, and then

$$\left\{ \begin{array}{l} \frac{1}{M} \sum_{k=1}^M h(\mathbf{\Lambda}_k) \frac{p_{\mathbf{\Lambda}}(\mathbf{\Lambda}_k \mid \boldsymbol{\alpha})}{p_{\mathbf{\Lambda}}(\mathbf{\Lambda}_k \mid \boldsymbol{\alpha}_{\ell}^*)} \xrightarrow[M \rightarrow \infty]{\text{a.s.}} I_1, \\ \frac{1}{M} \sum_{k=1}^M \frac{p_{\mathbf{\Lambda}}(\mathbf{\Lambda}_k \mid \boldsymbol{\alpha})}{p_{\mathbf{\Lambda}}(\mathbf{\Lambda}_k \mid \boldsymbol{\alpha}_{\ell}^*)} \xrightarrow[M \rightarrow \infty]{\text{a.s.}} I_2. \end{array} \right. \quad (\text{D.2})$$

Then it comes

$$\hat{E}_M^{\boldsymbol{\alpha}_{\ell}^*} (h(\mathbf{\Lambda}), \boldsymbol{\alpha}) \xrightarrow[M \rightarrow \infty]{\text{a.s.}} \mathbb{E}(h(\mathbf{\Lambda}) \mid \boldsymbol{\alpha}, \mathbf{y}_{1,\text{obs}}) \quad (\text{D.3})$$

Appendix D.1.2 Almost sure convergence of $\int_{\mathcal{A}} \hat{E}_M^{\boldsymbol{\alpha}_{\ell}^} (h(\mathbf{\Lambda}), \boldsymbol{\alpha}) \hat{p}_L^{\boldsymbol{\alpha}_{\ell}^*} (\boldsymbol{\alpha} \mid \mathbf{y}_{1,\text{obs}}) d\boldsymbol{\alpha}$ to*

$$\int_{\mathcal{A}} \mathbb{E}(h(\mathbf{\Lambda}) \mid \boldsymbol{\alpha}, \mathbf{y}_{1,\text{obs}}) \hat{p}_L^{\boldsymbol{\alpha}_{\ell}^*} (\boldsymbol{\alpha} \mid \mathbf{y}_{1,\text{obs}}) d\boldsymbol{\alpha}.$$

$\forall M \in \mathbb{N}, \forall \boldsymbol{\alpha} \in \mathcal{A}, \forall 1 \leq a \leq r,$

$$\frac{\partial \hat{E}_M^{\boldsymbol{\alpha}_{\ell}^*} (h(\mathbf{\Lambda}), \boldsymbol{\alpha})}{\partial \alpha_a} = \frac{1}{\left(\sum_{k=1}^M \frac{p_{\mathbf{\Lambda}}(\mathbf{\Lambda}_k \mid \boldsymbol{\alpha})}{p_{\mathbf{\Lambda}}(\mathbf{\Lambda}_k \mid \boldsymbol{\alpha}_{\ell}^*)} \right)^2} \times \left(\sum_{k=1}^M h(\mathbf{\Lambda}_k) \frac{\frac{\partial p_{\mathbf{\Lambda}}(\mathbf{\Lambda}_k \mid \boldsymbol{\alpha})}{\partial \alpha_a}}{p_{\mathbf{\Lambda}}(\mathbf{\Lambda}_k \mid \boldsymbol{\alpha}_{\ell}^*)} \sum_{k=1}^M \frac{p_{\mathbf{\Lambda}}(\mathbf{\Lambda}_k \mid \boldsymbol{\alpha})}{p_{\mathbf{\Lambda}}(\mathbf{\Lambda}_k \mid \boldsymbol{\alpha}_{\ell}^*)} - \sum_{k=1}^M h(\mathbf{\Lambda}_k) \frac{p_{\mathbf{\Lambda}}(\mathbf{\Lambda}_k \mid \boldsymbol{\alpha})}{p_{\mathbf{\Lambda}}(\mathbf{\Lambda}_k \mid \boldsymbol{\alpha}_{\ell}^*)} \sum_{k=1}^M \frac{\frac{\partial p_{\mathbf{\Lambda}}(\mathbf{\Lambda}_k \mid \boldsymbol{\alpha})}{\partial \alpha_a}}{p_{\mathbf{\Lambda}}(\mathbf{\Lambda}_k \mid \boldsymbol{\alpha}_{\ell}^*)} \right)$$

Then, $\forall M \in \mathbb{N},$

$$\bigcap_{k=1}^M \{ \mathbf{\Lambda}_k \in \mathcal{K} \} \subset \left\{ \forall \boldsymbol{\alpha} \in \mathcal{A}, \forall 1 \leq a \leq r, \left| \frac{\partial \hat{E}_M^{\boldsymbol{\alpha}_{\ell}^*} (h(\mathbf{\Lambda}), \boldsymbol{\alpha})}{\partial \alpha_a} \right| \leq 2b_0 \left| \frac{\sum_{k=1}^M \frac{\frac{\partial p_{\mathbf{\Lambda}}(\mathbf{\Lambda}_k \mid \boldsymbol{\alpha})}{\partial \alpha_a}}{p_{\mathbf{\Lambda}}(\mathbf{\Lambda}_k \mid \boldsymbol{\alpha}_{\ell}^*)}}{\sum_{k=1}^M \frac{p_{\mathbf{\Lambda}}(\mathbf{\Lambda}_k \mid \boldsymbol{\alpha})}{p_{\mathbf{\Lambda}}(\mathbf{\Lambda}_k \mid \boldsymbol{\alpha}_{\ell}^*)}} \right| \leq 2b_0 \frac{b_2 b_4}{b_3^2} \right\}.$$

Finally, we have

- $\forall \boldsymbol{\alpha} \in \mathcal{A}, \hat{E}_M^{\boldsymbol{\alpha}_{\ell}^*} (h(\mathbf{\Lambda}), \boldsymbol{\alpha}) \xrightarrow[M \rightarrow \infty]{\text{a.s.}} \mathbb{E}(h(\mathbf{\Lambda}) \mid \boldsymbol{\alpha}, \mathbf{y}_{1,\text{obs}})$

- $\mathbb{P} \left(\forall M \in \mathbb{N}, \bigcap_{k=1}^M \{ \mathbf{\Lambda}_k \in \mathcal{K} \} \right) = 1$ and then

- $\mathbb{P} \left(\forall M \in \mathbb{N}, \boldsymbol{\alpha} \mapsto \hat{E}_M^{\boldsymbol{\alpha}_{\ell}^*} (h(\mathbf{\Lambda}), \boldsymbol{\alpha}) \text{ is continuous on } \mathcal{A} \right) = 1$ from the continuity of $p(\boldsymbol{\lambda} \mid \cdot)$ for $\boldsymbol{\lambda} \in \mathcal{K}$.

- $\mathbb{P} \left(\forall M \in \mathbb{N}, \forall \boldsymbol{\alpha} \in \mathcal{A}, \forall 1 \leq a \leq r, \left| \frac{\partial \hat{E}_M^{\boldsymbol{\alpha}_\ell^*} (h(\boldsymbol{\Lambda}), \boldsymbol{\alpha})}{\partial \alpha_a} \right| \leq 2b_0 \frac{b_2 b_4}{b_3^2} \right) = 1.$
- $\mathbb{P} \left(\forall M \in \mathbb{N}, \forall \boldsymbol{\alpha} \in \mathcal{A}, \left| \hat{E}_M^{\boldsymbol{\alpha}_\ell^*} (h(\boldsymbol{\Lambda}), \boldsymbol{\alpha}, \boldsymbol{\omega}) \hat{p}_L^{\boldsymbol{\alpha}_\ell^*} (\boldsymbol{\alpha} \mid \mathbf{y}_{1,\text{obs}}) \right| \leq b_0 \times \hat{p}_L^{\boldsymbol{\alpha}_\ell^*} (\boldsymbol{\alpha} \mid \mathbf{y}_{1,\text{obs}}) \right) = 1.$
- $\boldsymbol{\alpha} \mapsto \mathbb{E}(h(\boldsymbol{\Lambda}) \mid \boldsymbol{\alpha}, \mathbf{y}_{1,\text{obs}}) = \frac{\int_{\mathcal{K}} h(\boldsymbol{\lambda}) p(\mathbf{y}_{1,\text{obs}} \mid \boldsymbol{\lambda}) \frac{p_{\boldsymbol{\Lambda}}(\boldsymbol{\lambda} \mid \boldsymbol{\alpha})}{p_{\boldsymbol{\Lambda}}(\boldsymbol{\lambda} \mid \boldsymbol{\alpha}_\ell^*)} p_{\boldsymbol{\Lambda}}(\boldsymbol{\lambda} \mid \boldsymbol{\alpha}_\ell^*) d\boldsymbol{\lambda}}{\int_{\mathcal{K}} p(\mathbf{y}_{1,\text{obs}} \mid \boldsymbol{\lambda}) \frac{p_{\boldsymbol{\Lambda}}(\boldsymbol{\lambda} \mid \boldsymbol{\alpha})}{p_{\boldsymbol{\Lambda}}(\boldsymbol{\lambda} \mid \boldsymbol{\alpha}_\ell^*)} p_{\boldsymbol{\Lambda}}(\boldsymbol{\lambda} \mid \boldsymbol{\alpha}_\ell^*) d\boldsymbol{\lambda}}$ is continuous on \mathcal{A} as
 - $\forall \boldsymbol{\alpha} \in \mathcal{A}, \boldsymbol{\lambda} \mapsto p(\mathbf{y}_{1,\text{obs}} \mid \boldsymbol{\lambda}) \frac{p_{\boldsymbol{\Lambda}}(\boldsymbol{\lambda} \mid \boldsymbol{\alpha})}{p_{\boldsymbol{\Lambda}}(\boldsymbol{\lambda} \mid \boldsymbol{\alpha}_\ell^*)} p_{\boldsymbol{\Lambda}}(\boldsymbol{\lambda} \mid \boldsymbol{\alpha}_\ell^*)$ and h are continuous almost everywhere on \mathcal{K} .
 - $\forall \boldsymbol{\lambda} \in \mathcal{K}, \boldsymbol{\alpha} \mapsto p_{\boldsymbol{\Lambda}}(\boldsymbol{\lambda} \mid \boldsymbol{\alpha})$ is continuous on \mathcal{A} .
 - $\forall \boldsymbol{\lambda} \in \mathcal{K}, \forall \boldsymbol{\alpha} \in \mathcal{A}, |h(\boldsymbol{\lambda}) p(\mathbf{y}_{1,\text{obs}} \mid \boldsymbol{\lambda}) p_{\boldsymbol{\Lambda}}(\boldsymbol{\lambda} \mid \boldsymbol{\alpha})| \leq b_0 b_1 b_2$, and $|p(\mathbf{y}_{1,\text{obs}} \mid \boldsymbol{\lambda}) p_{\boldsymbol{\Lambda}}(\boldsymbol{\lambda} \mid \boldsymbol{\alpha})| < b_1 b_2$ with $b_1 b_2$ and $b_0 b_1 b_2$ integrable on \mathcal{K} .

Then, from Theorem 2,

$$\int_{\mathcal{A}} \hat{E}_M^{\boldsymbol{\alpha}_\ell^*} (h(\boldsymbol{\Lambda}), \boldsymbol{\alpha}) \hat{p}_L^{\boldsymbol{\alpha}_\ell^*} (\boldsymbol{\alpha} \mid \mathbf{y}_{1,\text{obs}}) d\boldsymbol{\alpha} \xrightarrow[M \rightarrow \infty]{a.s.} \int_{\mathcal{A}} \mathbb{E}(h(\boldsymbol{\Lambda}) \mid \boldsymbol{\alpha}, \mathbf{y}_{1,\text{obs}}) \hat{p}_L^{\boldsymbol{\alpha}_\ell^*} (\boldsymbol{\alpha} \mid \mathbf{y}_{1,\text{obs}}) d\boldsymbol{\alpha}$$

Appendix D.1.3 Almost sure convergence of $\hat{E}_{N,M}^{\boldsymbol{\alpha}_\ell^} (h(\boldsymbol{\Lambda}))$ to $\int_{\mathcal{A}} \hat{E}_M^{\boldsymbol{\alpha}_\ell^*} (h(\boldsymbol{\Lambda}), \boldsymbol{\alpha}) \hat{p}_L^{\boldsymbol{\alpha}_\ell^*} (\boldsymbol{\alpha} \mid \mathbf{y}_{1,\text{obs}}) d\boldsymbol{\alpha}$ for a given M .*

Again, MCMC sampling provides $(\mathbf{A}_i)_{i=1}^N$ a Harris ergodic Markov Chain with invariant distribution $\hat{p}_L^{\boldsymbol{\alpha}_\ell^*} (\boldsymbol{\alpha} \mid \mathbf{y}_{1,\text{obs}})$. It directly comes [39]

$$\hat{E}_{N,M}^{\boldsymbol{\alpha}_\ell^*} (h(\boldsymbol{\Lambda})) = \frac{1}{N} \sum_{i=1}^N \hat{E}_M^{\boldsymbol{\alpha}_\ell^*} (h(\boldsymbol{\Lambda}), \mathbf{A}_i) \xrightarrow[N \rightarrow \infty]{a.s.} \int_{\mathcal{A}} \hat{E}_M^{\boldsymbol{\alpha}_\ell^*} (h(\boldsymbol{\Lambda}), \boldsymbol{\alpha}) \hat{p}_L^{\boldsymbol{\alpha}_\ell^*} (\boldsymbol{\alpha} \mid \mathbf{y}_{1,\text{obs}}) d\boldsymbol{\alpha} \quad (\text{D.4})$$

Appendix D.1.4 Conclusion on $\lim_{M \rightarrow \infty} \lim_{N \rightarrow \infty} \hat{E}_{N,M}^{\boldsymbol{\alpha}_\ell^} (h(\boldsymbol{\Lambda}))$.*

From the previous sections, we have

$$\left\{ \begin{array}{l} \hat{E}_{N,M}^{\boldsymbol{\alpha}_\ell^*} (h(\boldsymbol{\Lambda})) \xrightarrow[N \rightarrow \infty]{a.s.} \int_{\mathcal{A}} \hat{E}_M^{\boldsymbol{\alpha}_\ell^*} (h(\boldsymbol{\Lambda}), \boldsymbol{\alpha}) \hat{p}_L^{\boldsymbol{\alpha}_\ell^*} (\boldsymbol{\alpha} \mid \mathbf{y}_{1,\text{obs}}) d\boldsymbol{\alpha} \\ \int_{\mathcal{A}} \hat{E}_M^{\boldsymbol{\alpha}_\ell^*} (h(\boldsymbol{\Lambda}), \boldsymbol{\alpha}) \hat{p}_L^{\boldsymbol{\alpha}_\ell^*} (\boldsymbol{\alpha} \mid \mathbf{y}_{1,\text{obs}}) d\boldsymbol{\alpha} \xrightarrow[M \rightarrow \infty]{a.s.} \int_{\mathcal{A}} \mathbb{E}(h(\boldsymbol{\Lambda}) \mid \boldsymbol{\alpha}, \mathbf{y}_{1,\text{obs}}) \hat{p}_L^{\boldsymbol{\alpha}_\ell^*} (\boldsymbol{\alpha} \mid \mathbf{y}_{1,\text{obs}}) d\boldsymbol{\alpha} \end{array} \right.$$

It leads to

$$\mathbb{P} \left(\lim_{M \rightarrow \infty} \lim_{N \rightarrow \infty} \hat{E}_{N,M}^{\boldsymbol{\alpha}_\ell^*} (h(\boldsymbol{\Lambda})) = \int_{\mathcal{A}} \mathbb{E}(h(\boldsymbol{\Lambda}) \mid \boldsymbol{\alpha}, \mathbf{y}_{1,\text{obs}}) \hat{p}_L^{\boldsymbol{\alpha}_\ell^*} (\boldsymbol{\alpha} \mid \mathbf{y}_{1,\text{obs}}) d\boldsymbol{\alpha} \right) = 1 \quad \square$$

Appendix D.2 Almost sure $\lim_{N \rightarrow \infty} \lim_{M \rightarrow \infty} \hat{E}_{N,M}^{\boldsymbol{\alpha}_\ell^*} (h(\boldsymbol{\Lambda}))$

From Equation (D.3), we have

$$\forall \boldsymbol{\alpha} \in \mathcal{A}, \hat{E}_M^{\boldsymbol{\alpha}_\ell^*} (h(\boldsymbol{\Lambda}), \boldsymbol{\alpha}) \xrightarrow[M \rightarrow \infty]{a.s.} \mathbb{E}(h(\boldsymbol{\Lambda}) \mid \boldsymbol{\alpha}, \mathbf{y}_{1,\text{obs}})$$

It leads to

$$\hat{E}_{N,M}^{\alpha_\ell^*}(h(\Lambda)) = \frac{1}{N} \sum_{i=1}^N \hat{E}_M^{\alpha_\ell^*}(h(\Lambda), \mathbf{A}_i) \xrightarrow[M \rightarrow \infty]{a.s.} \frac{1}{N} \sum_{i=1}^N \mathbb{E}(h(\Lambda) \mid \mathbf{A}_i, \mathbf{y}_{1,\text{obs}})$$

And similarly to Equation (D.4),

$$\frac{1}{N} \sum_{i=1}^N \mathbb{E}(h(\Lambda) \mid \mathbf{A}_i, \mathbf{y}_{1,\text{obs}}) \xrightarrow[N \rightarrow \infty]{a.s.} \int_{\mathcal{A}} \mathbb{E}(h(\Lambda) \mid \boldsymbol{\alpha}, \mathbf{y}_{1,\text{obs}}) \hat{p}_L^{\alpha_\ell^*}(\boldsymbol{\alpha} \mid \mathbf{y}_{1,\text{obs}}) d\boldsymbol{\alpha},$$

Finally,

$$\mathbb{P} \left(\lim_{N \rightarrow \infty} \lim_{M \rightarrow \infty} \hat{E}_{N,M}^{\alpha_\ell^*}(h(\Lambda)) = \int_{\mathcal{A}} \mathbb{E}(h(\Lambda) \mid \boldsymbol{\alpha}, \mathbf{y}_{1,\text{obs}}) \hat{p}_L^{\alpha_\ell^*}(\boldsymbol{\alpha} \mid \mathbf{y}_{1,\text{obs}}) d\boldsymbol{\alpha} \right) = 1 \quad \square$$

Appendix E. EMBEDDED DISCREPANCY

This section is just a brief recall of the work of [13]. Their idea is to consider an embedded random discrepancy δ , parameterized by λ^2 . In the following, this discrepancy is denoted $\delta(\Lambda^2, \Xi)$, where Ξ highlights explicitly the stochastic dimension.

This formulation leads to considering the random output $f_t(\mathbf{x}, \lambda^1 + \delta(\lambda^2, \Xi))$, where $\lambda^1 + \delta(\lambda^2, \Xi)$ is a random variable parameterized by λ^1 and λ^2 . The problem is treated as a Bayesian estimation of the parameters λ^1 and λ^2 , that are parameters of a pdf. In the following, we denote $\tilde{\lambda} = (\lambda^1, \lambda^2)$ the set of augmented parameters. Then, we consider with the GP formulation

$$Y_t(\mathbf{x}) = \hat{f}_t(\mathbf{x}, \Lambda^1 + \delta(\Lambda^2, \Xi)) + \sqrt{v_1(\mathbf{x}, \Lambda^1 + \delta(\Lambda^2, \Xi))} E^f,$$

with $\Lambda^1 \in \mathbb{R}^q$, $\Lambda^2 \in \mathbb{R}^q$.

Appendix E.1 Likelihood estimation.

We need to investigate $p(\mathbf{y}_{1,\text{obs}} \mid \tilde{\lambda})$ the likelihood of $\tilde{\lambda}$. We first define the random vectors

$$\begin{cases} \hat{\mathbf{F}}(\tilde{\lambda}) = \left(\hat{f}_1(\mathbf{x}_j, \lambda^1 + \delta(\lambda^2, \Xi)) \right)_{j=1}^n \\ \mathbf{H}(\tilde{\lambda}) = \left(\hat{f}_1(\mathbf{x}_j, \lambda^1 + \delta(\lambda^2, \Xi)) + \sqrt{v_1(\mathbf{x}_j, \lambda^1 + \delta(\lambda^2, \Xi))} E^f + E_j \right)_{j=1}^n \end{cases}$$

Then, we have

$$p(\mathbf{y}_{1,\text{obs}} \mid \tilde{\lambda}) = \pi_{\mathbf{H}(\tilde{\lambda})}(\mathbf{y}_{1,\text{obs}})$$

with $\pi_{\mathbf{H}(\tilde{\lambda})}$ the pdf of $\mathbf{H}(\tilde{\lambda})$. One challenge is to evaluate $\pi_{\mathbf{H}(\tilde{\lambda})}$ for every $\tilde{\lambda}$. A high dimensional Kernel Density Estimation (KDE, [40]) would provide a precise computation but is too costly in our context. Several likelihood approximations are proposed in [13], and we have decided to work with an independent normal approximation here, for simplicity reasons. The idea is to get R samples $(\boldsymbol{\xi}_r)_{r=1}^R$ that are i.i.d. realizations of the random variable Ξ , and then compute for $1 \leq j \leq n$

$$\begin{cases} \hat{\mu}_j &= \frac{1}{R} \sum_{r=1}^R \hat{f}_1(\mathbf{x}_j, \lambda^1 + \delta(\lambda^2, \boldsymbol{\xi}_r)) \\ \hat{\sigma}_j^2 &= \frac{1}{R-1} \sum_{r=1}^R (\hat{f}_1(\mathbf{x}_j, \lambda^1 + \delta(\lambda^2, \boldsymbol{\xi}_r)) - \hat{\mu}_j)^2 + \frac{1}{R} \sum_{r=1}^R v_1(\mathbf{x}_j, \lambda^1 + \delta(\lambda^2, \boldsymbol{\xi}_r)) + \sigma_\varepsilon^2 \end{cases}$$

Finally, with the independent normal approximation, the pdf $\pi_{\mathbf{H}(\tilde{\lambda})}$ is defined as

$$\pi_{\mathbf{H}(\tilde{\lambda})}(\mathbf{y}) = \prod_{j=1}^n \frac{1}{\sqrt{2\pi\hat{\sigma}_j^2}} \exp\left(-\frac{(y_j - \hat{\mu}_j)^2}{2\hat{\sigma}_j^2}\right).$$

Appendix E.2 Polynomial chaos representation.

The random discrepancy $\delta(\lambda^2, \Xi)$ needs to be parametrized. As presented in [13], we have opted for a Polynomial Chaos (PC, [41]) representation, and more precisely Legendre-Uniform PC that can respect the support of the calibration parameters. It gives

$$\lambda^1 + \delta(\lambda^2, \Xi) = \lambda^1 + \text{diag}(\lambda^2 \Xi^T)$$

with $\Xi_i \sim \mathcal{U}(-1, 1)$, $1 \leq i \leq q$ and $\Xi_i \perp \Xi_j$ if $i \neq j$.

Appendix E.3 Prior construction.

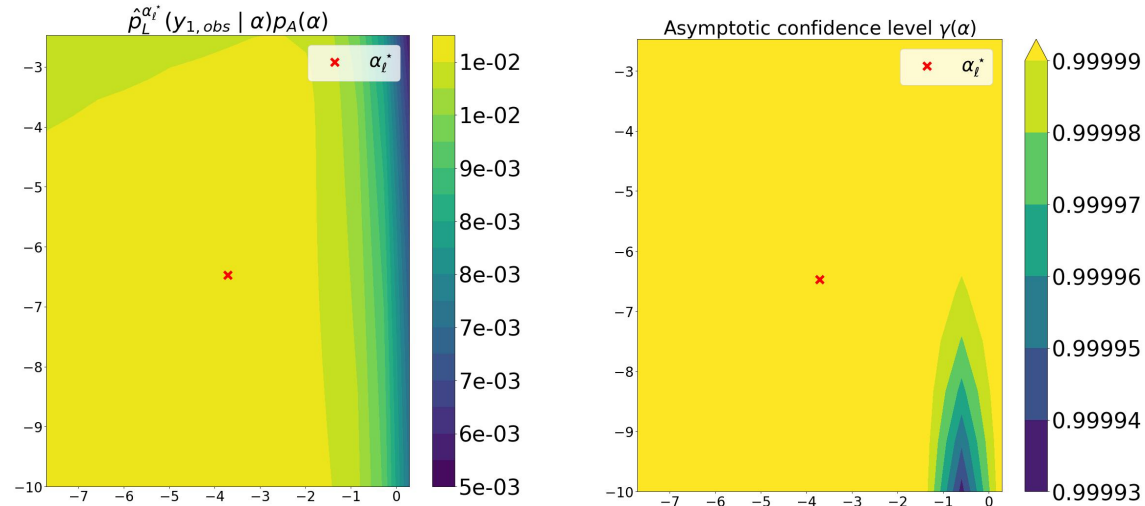
The choice of the prior is here driven by the respect of the support of the parameters once again. We have opted for the uniform prior that respects the constraints $\lambda_i^1 - \lambda_i^2 \geq 0$ and $\lambda_i^1 + \lambda_i^2 \leq 1$, and $\lambda_i^2 \geq 0$ as well to avoid bimodal distributions. We then have

$$p_{(\Lambda^1, \Lambda^2)}(\lambda^1, \lambda^2) \propto \prod_{i=1}^q 1_{\lambda_i^2 > 0} 1_{\lambda_i^1 - \lambda_i^2 > 0} 1_{\lambda_i^1 + \lambda_i^2 < 1}.$$

Appendix E.4 Computation cost.

This strategy is relevant in our context but involves a high computation cost compared to the method presented in this article. Indeed, computing the likelihood for a single λ requires $R \times n$ calls to the simulator (or the surrogate model), compared to n calls in our method. This is a major difference as R is associated with sampling in dimension q and thus must be large.

Appendix F. POSTERIOR DISTRIBUTION AND MAP FOR α



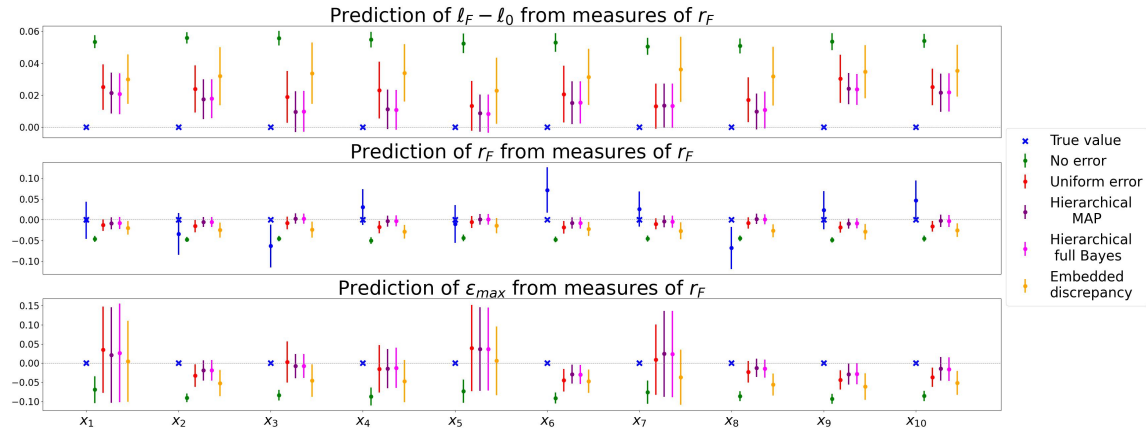
(a) Estimated unnormalized posterior distribution $\hat{p}_L^{\alpha_i^*}(\mathbf{y}_{1, \text{obs}} | \alpha) p_A(\alpha)$.

(b) Asymptotic confidence level $\gamma(\alpha)$ associated with $p(\alpha | \mathbf{y}_{1, \text{obs}}) < 1.05p(\alpha_i^* | \mathbf{y}_{1, \text{obs}})$

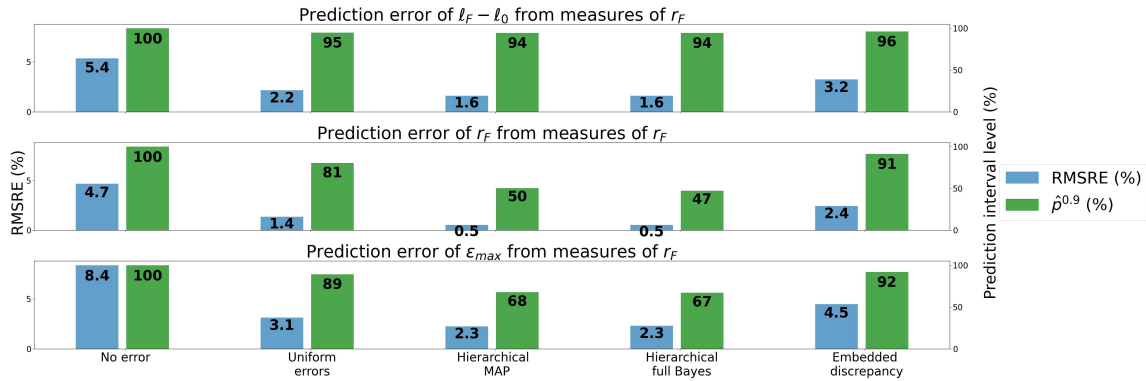
Figure F.7: Illustration of the estimation of the posterior distribution $p(\alpha | \mathbf{y}_{1, \text{obs}})$ (Figure F.7a) and the confidence level $\gamma(\alpha)$ associated to $p(\alpha | \mathbf{y}_{1, \text{obs}}) < 1.05p(\alpha_i^* | \mathbf{y}_{1, \text{obs}})$ (Figure F.7b) with $y_1 = \epsilon_{\text{max}}$ for the prediction at \mathbf{x}_6 .

Appendix G. EXAMPLE OF RESULTS WITH SMALLER NOISE

Figure G.8 shows the results obtained from measurements of r_f with a noise standard deviation of 0.3, instead of 0.9 in the core of the article. The difference between the *Uniform error* approach and the two hierarchical model-based methods is less pronounced, as the prior has a reduced influence.



(a) Mean and standard deviation of the normalized posterior distribution $\frac{Y_t(\mathbf{x}_j) - y_t(\mathbf{x}_j)}{y_t(\mathbf{x}_j)} \mid \mathbf{y}_{1,\text{obs}}^{-j}$, $1 \leq j \leq 10$, with $y_1 = r_f$, compared to the true values $y_t(\mathbf{x}_j)$ shifted to 0 shown as blue crosses for $1 \leq t \leq 3$. The measurement of r_f is indicated by the blue dot, with its standard deviation represented by the associated error bar.



(b) Performance metrics from observations of r_f . The blue bar is the RMSRE in %, while the green bar represent $\hat{p}_{t,N,M}^{0.9}$ in %, the 0.9 quantile of the aggregated levels of the smallest prediction intervals.

Figure G.8: Prediction of the three outputs from observations of r_f , with a standard deviation of 0.3 for the measurement noise.